EUROPEAN COMMISSION
DIRECTORATE-GENERAL
Joint Research Centre

A SYNOPTIC VIEW OF CARBON AND OXYGEN DYNAMICS IN EUROPEAN REGIONAL SEAS: AN APPROACH COUPLING MODELLED AND SATELLITE DATASETS
PART A: CONCEPTUAL MODEL AND SENSITIVITY ANALYSIS

LAURENCE DEYDIER-STEPHAN, ADOLF STIPS, MARK DOWELL, JUDITH CHALLIS & WOLFRAM SCHRIMPF

2005 **EUR 21813 EN**

EUROPEAN COMMISSION
DIRECTORATE-GENERAL
Joint Research Centre

Institute for Environment and Sustainability

A SYNOPTIC VIEW OF CARBON AND OXYGEN DYNAMICS IN EUROPEAN REGIONAL SEAS: AN APPROACH COUPLING MODELLED AND SATELLITE DATASETS
PART A: CONCEPTUAL MODEL AND SENSITIVITY ANALYSIS

LAURENCE DEYDIER-STEPHAN, ADOLF STIPS, MARK DOWELL, JUDITH CHALLIS & WOLFRAM SCHRIMPF

July 2005

European Commission- Joint Research Centre
Institute for Environment and Sustainability
Inland & Marine Waters Unit
TP 272, I-21021 ISPRA (VA)- Italy

2005 **EUR 21813 EN**

LEGAL NOTICE

A great deal of additional information on the
European Union is available on the Internet.
It can be accessed through the Europa server
(http://europa.eu.int)

EUR 21813 EN

Printed in Italy

ABSTRACT

A major work package of the JRC/IES FP6 Action 2121 ECOMAR is related to the further development and validation of ecological indices and the development of value added products of state and process of coastal and marine ecosystems in European regional seas. In this context a specific task is to develop, apply and validate a model for the quantification of oxygen and carbon cycles in shallow coastal waters exposed or sensitive to eutrophication. This model should be used for a more accurate quantification of oxygen depletion risk at a pan-European level.

In this report the development of an accurate model for oxygen and carbon cycles in shelf and eutrophicated areas is presented. Following the recent development of eutrophication indices for coastal and marine areas, OXYRISK and PSA, and several recent attempts to implement a thorough but simple coupled benthic/pelagic model, the new model is applied in highly eutrophicated and sensitive coastal areas of the European seas. A new approach is proposed coupling a 3D hydrodynamic and a 1D ecosystem model, supplied with primary production data derived from satellite remote sensing. This approach allows getting a synoptic view in time and space of carbon and dissolved oxygen concentrations for different basins. A first application of the model is made for the Baltic Sea. The biogeochemical sub-model includes coupled benthic/pelagic processes specifically addressing oxygen quantification in the sediment, as in the benthic and upper layers of the water column. This ecosystem model will be gradually developed further from a simple (POC)/(DO) model into a NPZD/sediment model, while being fully coupled with the hydrodynamic model for advection and diffusion processes. The model will be validated along with its application as an eutrophication assessment tool for European seas.

I-INTRODUCTION & OBJECTIVES

The concept of eutrophication developed and applied from the Sixties in freshwater and lakes, has been specifically applied to seas and coastal waters only during the last 20 years with long-term experiments and developments of specific definitions and indices for the assessment of ecosystems (Vollenweider, 1992; Riegman, 1995; Justic *et al*., 2002). Following these specific developments and experiments of marine eutrophication some indices were developed like TRIX (Vollenweider *et al*., 1998) and others (Rice, 2003, Kabuta & Laane, 2003), considering biological, chemical and physical parameters, for application of ecological indices (Karydis & Tsirtsis, 1996) in different coastal ecosystems and assessments of eutrophication and trophic states (Rabalais &Turner, 2001, Moncheva *et al.*, 2002 a,b, Denmann, 2003,). An attempt for a general definition and concept of eutrophication and ecological indices resulted (Nixon, 1995) in the definition of eutrophication as the "increase in the rate of supply of organic matter to an ecosystem" and Cloern's concept (2001) for the quantification and development of eutrophication indices in ecosystems. In parallel to these experiments and indices, different models were developed for eutrophication assessment in marine areas and marine ecosystem models, were set up like ERGOM (Neumann, 2000, Neumann *et al.*, 2002) for the Baltic Sea, and ERSEMv3 applied in the North Sea as well as in the Adriatic Sea (Moll & Radach, 2003, Vichi *et al.,* 2003). Others regional models emerged, more specific for rivers and estuaries (Borsuk *et al.*, 2001,a,b, 2004) as WASP6 of Wood *et al,.* (2003), or Turner *et al.*, (2005), for the Neuse and Mississipi river estuaries (Paerl *et al.,* 1998), Zaldivar *et al.* (2003) and Tett *et al.* (2003) for European lagoons, fjord and costal areas (Hamersley & Howes, 2003). These different type of models share the quantification of oxygen together with nutrients and phytoplankton/zooplankton or carbon cycles in water, seldomly on sediment.

Following the development of the PSA (Physical Sensitive Area) and OXYRISK (Oxygen depletion risk) index, respectively, capturing the impact of anthropogenic eutrophication for coastal areas ecosystems, the two indices (Druon *et al,.* 2002, 2004) were applied in different European regional seas. These indices were conceived for a more qualitative usage, while we built on a simple but quantitative model of eutrophication assessment, focused on some impacts: anoxia and hypoxia in sensitive or eutrophied shallow areas (depth less than 100m).

The model described in this report is elaborated for larger scale eutrophication processes and application in European regional seas. The resulting hydrodynamic/biogeochemical model is based on the carbon and oxygen cycles in water and sediment, as the sediment compartment constitutes an important element of shelf ecosystems and especially eutrophied ecosystems. Following Soetaert *et al.,* (2000) and their diagenetic sediment model interfacing a pelagic/sediment models for the nutrients, carbon and oxygen cycles (Soetaert *et al.* 1996, 2001),we have coupled the major but simplified processes in sediment for POC/DO to our biogeochemical model. The model used for provision of the required hydrodynamic data is the 3D physical model GETM (Burchard & Bolding, 2002) developed in house and validated for the North Sea and Baltic Sea. Finally, the main innovative feature of this model is the provision of primary production derived from satellite remote sensing.

The original algorithms have been developed for a better estimation of primary production in open oceans than in marginal or regional seas (Behrenfeld & Falkowski, 1997; Dowell *et al.,* 2005). With regard to the application areas (coastal/shallow waters) the

calculation of primary production is based on the SeaWIFS OC4V4 algorithm, adapted for coastal or land-influenced waters.

The 1D POC/DO model developed, the application area and a sensitive analysis are described in this report. Testing, calibration and validation of the coupled model will be performed in different sub-basins of the Baltic Sea, a shelf sea, largely and historically exposed to eutrophication and anoxia phenomena (Richardson & Jorgensen, 1996, Conley *et al.,* 2002, Carstensen *et al.,* 2003) but also in the Adriatic Sea and North Sea, aiming at fulfilling a range of bathymetry, advection and primary production conditions (Arhonditsis & Brett, 2004). This validation phase will be exposed in a second report.

II- MATERIALS AND METHODS

2.1 HYDRODYNAMICAL MODEL

The 3D hydrodynamic model used in this study is called GETM / General Estuarine Transport Model and has been developed and validated for the Baltic Sea and North Sea (Burchard & Bolding, 2002, Stips *et al.,* 2004). Meteorological parameters, such as winds, precipitation or evaporation provide the model forcing and it has a spatial horizontal discrete grid of 5.5 km. Typical variables computed by this model are water temperature, salinity, turbulent diffusivities, mixed layer and bottom layer thicknesses and bottom shear stress. These results are used as data or forcing functions in the biogeochemical model, together with the wind stress, coming from an ECMWF model. All these outputs are given bi-daily and used after an interpolation to obtain the same time-step and inputs for the biogeochemical model during the whole year run.

2.2 PRIMARY PRODUCTION MODEL/ALGORITHM

The model of primary production/algorithm used is suitable specifically for coastal waters, using remote sensing data and especially Chl-a, PAR, Kd, SST measurements. This model is integrated over the mixed layer, computed by the hydrodynamic model and is based on a formulation obtained through dimensional analysis by Platt and Sathyendranath (1993). The assignment of the photosynthetic parameters PBmax and Ek is achieved by the combined use of a temperature dependent relationship for the maximum growth rate (Eppley, 1972) and the use of variable formulation to retrieve the C: Chl ratio following the empirical relation of Cloern *et al.,* (1995).

2.3 CONCEPTUAL MODELING

Considering the different ecosystems models existing and their actual tendency, it was decided to build upon a simple but quantitative model for eutrophication impact assessment (Vidal *et al.,* 1999), following the DPSIR concept, especially for the oxygen depletion risk, in the coastal shelf areas. Inspired from the conceptual model (fig.1), the focus is first on pressure: (physics and nutrients), then on state: higher primary production and production of organic matter, for modelling some of the most visible and worst impact for the ecosystem state: oxygen deficiency. The parameterization of this model is done for a coupled 1D hydrodynamic-biogeochemical model supplied by PP derived from remote sensing data.

Similar to other, more or less complex, coupled hydrodynamic and biological models (Druon & LeFevre, 1999; Carlsson *et al.,* 1999; Cugier, 1999; Vichi *et al.*, 2003; Dadou *et al*., 2004), a NPZD model (including sources and sinks) is coupled with a 3D hydrodynamical models similar to those reviewed by Moll & Radach (2003) with the compulsory use of remote sensing data (Harding *et al.,* 1999). Following some recent developments of ecosystem modelling and eutrophication assessment, as OXYRISK (Djavidnia *et al*., 2005) and ERGOM (Neumann, 2000; Neumann *et al*., 2002) a 1D model is developed for Particulate Organic Carbon/ Dissolved Oxygen for coastal and marine areas exposed to eutrophication. Furthermore a ‘sediment box’ is added considering this compartment and its major processes interacting with the pelagic compartments (diagenetic benthic model,

Soetaert *et al.*, 1996b, 1998), but slightly simplified as recommended by Soetart *et al.* (2000) for carbon and oxygen sources and sinks. The equations are written for each compartment and state variable representing sources and sinks for carbon and oxygen, together with physical processes, such as diffusion (molecular and turbulent) and reaeration due to wind stress and bottom shear stress for oxygen dynamics. Hence, for each state variable POC and DO, the equations are solved for the mixed layer, the pycno layer the bottom layer and the sediment layer/compartments.

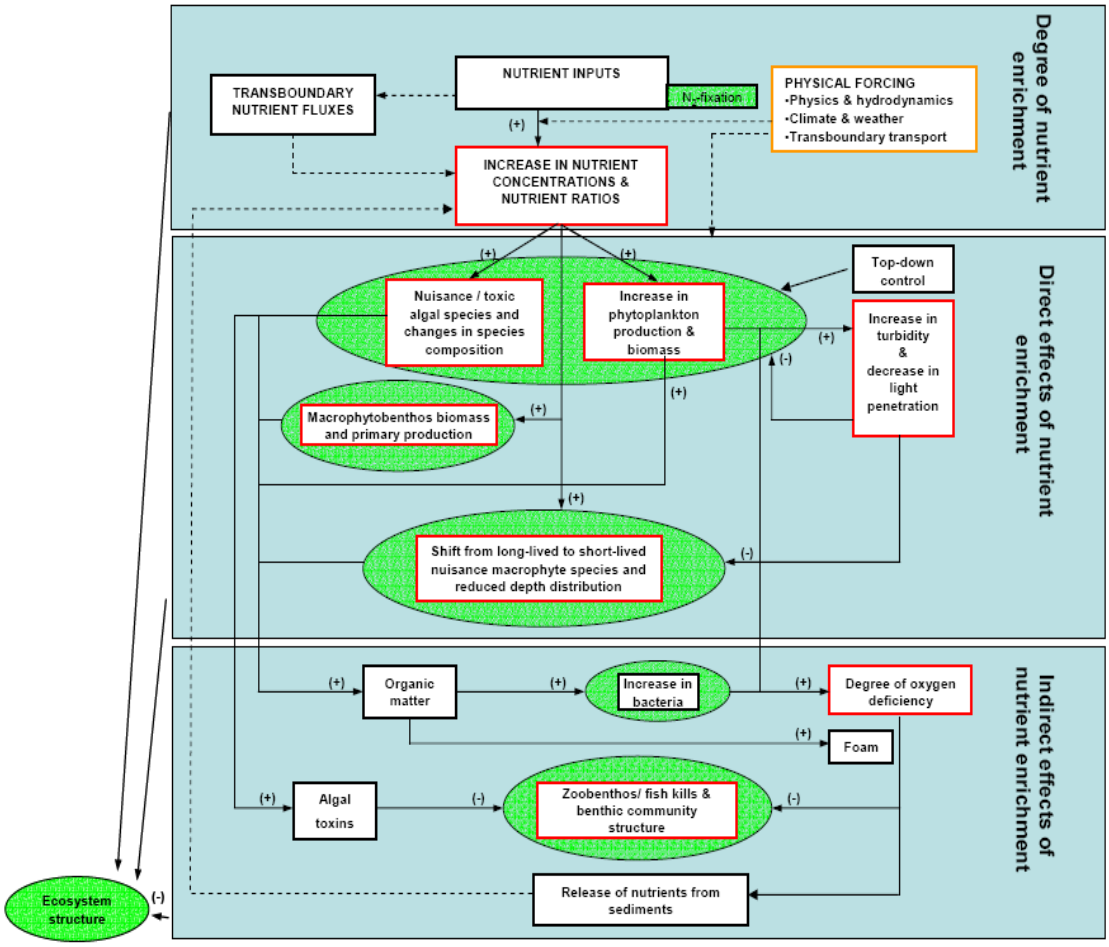

Figure 1: Conceptual model for assessing eutrophication in the European Seas linking nutrient enrichments and its direct and indirect effects in the ecosystem. The biological components are shadowed in green; the elements also used in the EC-Water Framework Directive are framed in red. This figure is an outcome of the European Commission-Joint Research Centre, Black Sea and Helsinki Commissions joint monitoring and assessment workshop (extract from http://sea.helcom.fi/dps/docs/folders/MONAS, BSC *et al.*, 2004).

2.4 COMPUTER PROGRAM

The numerical model as well as the data processing and analysis are made using the IDLv 6.1, software. Therefore, all data and results are processed and saved in IDL format for Windows or Linux applications.

2.5 SENSITIVITY ANALYSIS

Following, the ecosystem theory for building, calibrating and validating an accurate model (Jorgensen, 1992), a sensitivity analysis is compulsory, allowing the calculation of the sensitivity and correlation of the model components. Considering the uncertainty of the model, i.e. the addition of errors in measurements and lack of precision for parameter estimation and the final objective of this model to be applied on a pan-European scale, we performed a global sensitivity analysis, varying the value of each model components considered as a parameter, within the whole range of values found in the literature for biogeochemical models for estuaries, lagoons and shallow seas. The model sensitivity analysis is performed individually, varying each parameter one by one. Using the sensitivity formula of Friedrichs (2001), the sensitivity of the model parameters is evaluated for the different model components contained in our model. This formula is applied not only for fractional increase but also decrease, as the uncertainty evaluation is included in this global sensitivity analysis.
The sensitivity of a certain model component or variable C to a given model parameter X is defined as the fractional change in C due to a fractional change: i in the value of the parameter X.

$$S_{C,X} = \frac{\dfrac{C_X - C_{X\pm i}}{C_{X\pm i}}}{\dfrac{X - X_{\pm i}}{X_{\pm i}}}$$

Where C is the annual mean value of one of the eight components of the DOX/POC model, so namely oxygen concentrations and particulate organic carbon. The variables considered are: mixed layer, pycnocline layer, bottom layer and sediment layer.

2.6 VALIDATION SITES

In order to verify if this model for the oxygen cycle is valid, the equations and their applicability are verified using *in situ* data in different areas of the European Seas. Eventually, the model DO content will be calculated in some areas of the Baltic and North Sea but also in the Black and Mediterranean seas (Danube delta and Emilia-Romagna coast, respectively) and compared to *in situ* data in the chosen areas.

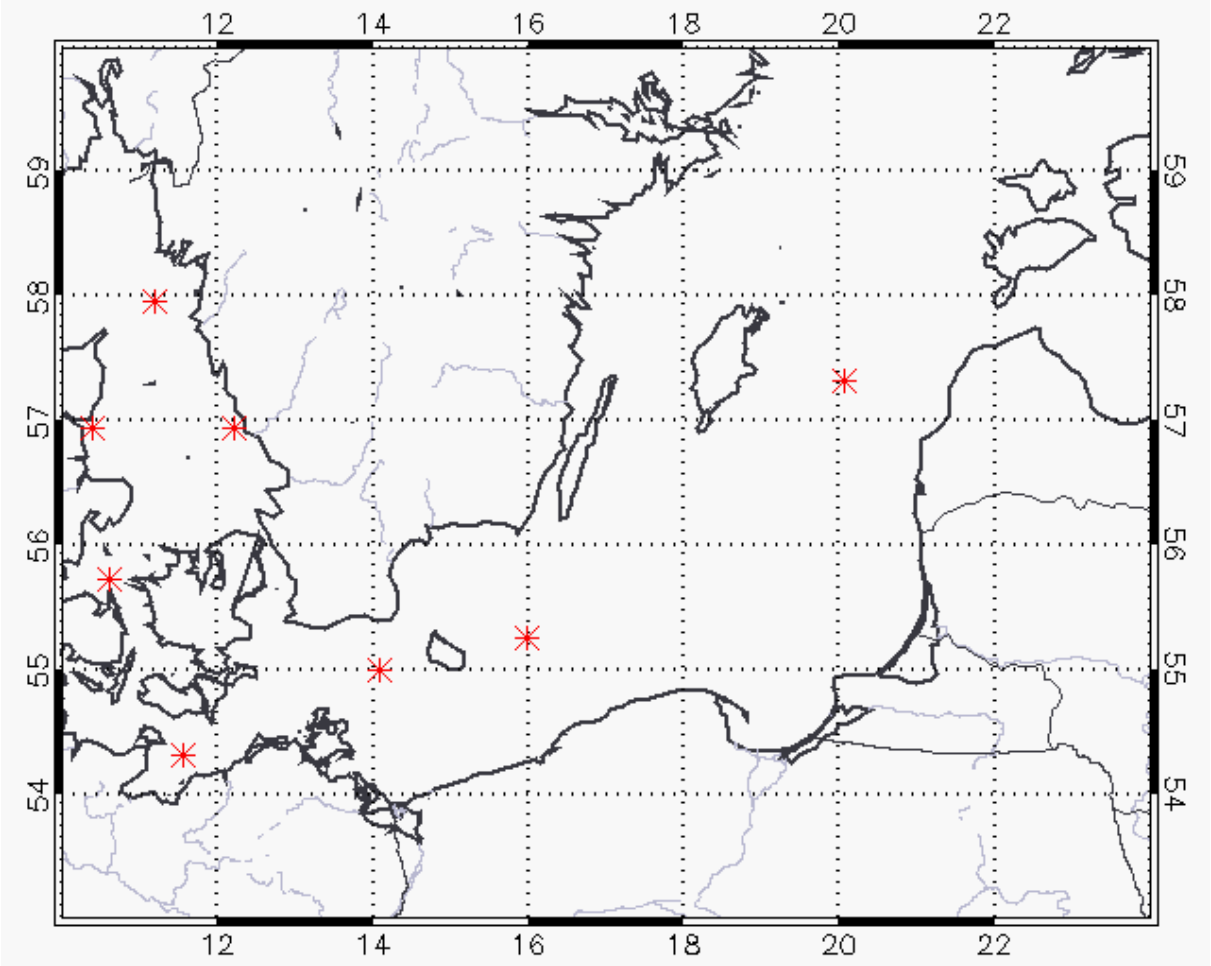

Figure 2: Baltic Sea with stations coordinates

From the Northern Kattegat: Fladen, Alborg, Anholt, to the Belt Sea, then Kiel Bight, Arkona and Bornholm Basins and finally in the Gotland Sea for the North East of the Baltic Proper.

III- BIOGEOCHEMICAL MODEL DESCRIPTION

3.1 CONCEPTUAL MODEL SKETCH

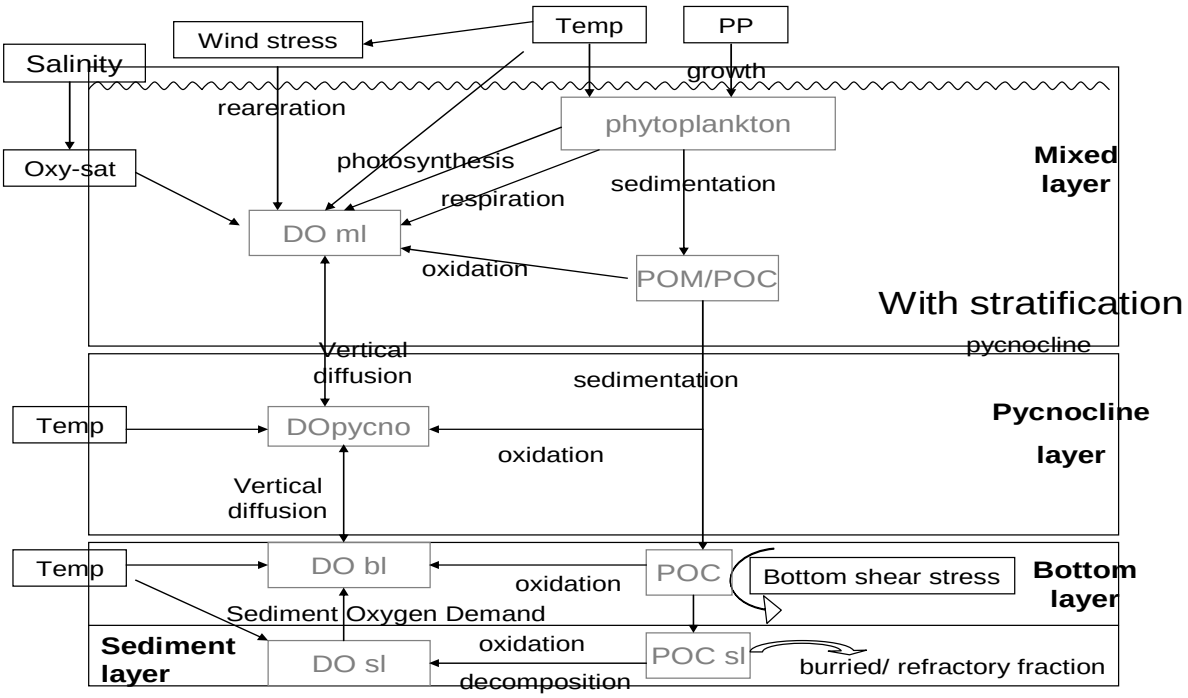

Figure 3: Schema of the conceptual biogeochemical model with inputs in the black boxes: temperature, salinity, wind and bottom shear stresses for hydrodynamic forcing functions and primary production inputs supplied by remote sensing data. State variables POC and DO are divided within grey boxes: ml, pl, bl and sl corresponding to dynamic properties: pycnocline depth for ml and pl (mixed and pycnocline layers) and specific properties considered in this model benthic parts: bottom layer (bl) and sediment layer (sl). Connectors represent the different physical and biogeochemical processes of production/consumption between state variables. For DO: reaeration, photosynthesis, respiration, oxidation of carbon by oxygen, vertical diffusion, plus oxidation and water-sediment diffusivity for the sediment and bottom layer. For POC: growth, oxidation, sedimentation, bottom shear stress and oxidation in sediment and the bottom layer.

3.2 MODEL EQUATIONS

Some of the physical data which are included in the model are computed before the run of the biogeochemical model as they are compulsory for model execution. Essentially, these data are used to calculate the oxygen saturation concentration in water, the reaeration rate and the pycnocline or mixed layer depth in the area chosen.

Calculation of the oxygen saturation concentration in the water (Weiss, 1970):

$$\text{Oxy-sat} = C1 \times \exp\left[A1 + A2(100/T) + A3\ln(T/100) + \text{sal}(B1 + B2(T/100) - B3(T/100)^2)\right]$$

With A1= -173.4292
A2= 249.6339
A3= 143.3483
A4= -21.8492
B1= -0.033096
B2= 0.014259
B3= 0.0017
C1= 1.426 (mg/l)
T = degree Kelvin + 273.15
Sal = salinitiy in PSU

This equation is used to calculate the saturation concentration of oxygen in water at each time step and for each layer. These concentrations of oxygen at saturation are further used for the reaeration component of the DO state variable.

Reaeration rate of the water column due to wind, or air/water exchange (O'Connor, 1983):

$K_2c_{(20\,^\circ C)} = 3.93\ V^{0.5}\ D^{-1.5}$
$K_2c(T) = K_{2\,(20\,^\circ C)}\ \Theta^{(T-20)}$

$K_{2\,(20\,^\circ C)}$ is the flow-induced reareration rate coefficient at 20 °C
K_{2c} (T) is the reareration rate coefficient at ambient temperature, per day^{-1}
$\Theta = 1{,}08$
V is the average wind velocity measured at 10m height, in m/sec, for the area considered, (for this study extracted from ECMWF model data)
D is the water depth in m

As for the oxygen saturation concentration, the parameter K_2c is calculated for each time step and for each layer of the stations simulated by the model.

Density calculated in the water column (UNESCO, 1981):

Based on the formula of density applied for salt water the densities of each layer are calculated using the output of the hydrodynamic model GETM:

$$\rho = \rho + \left(\left(C2 \times T + C1\right) \times T + C0\right) \times Sr + D0 \times S + \left(\left(\left(\left(B4 \times T + B3\right) \times T + B2\right) \times T + B1\right) \times T + B0\right) \times S$$

With S= salinity in PSU
T= temperature in °C
B0 = (8.24493e-1)
B1 = (-4.0899e-3)
B2 = (7.6438e-5)
B3 = (-8.2467e-7)

B4 = (5.3875e-9)
C0 = (-5.72466e-3)
C1 = (1.0227e-4)
C2 = (-1.6546e-6)
D0 = (4.8314e-4)
Sr = $\sqrt{|S|}$

Based on the calculation of the density for each layer ρ, the maximum differences between two following layers are calculated and the corresponding depth of the maximum density difference is identified as the mixed layer depth or pycnocline depth.

3.3 PARAMETERS AND FORCING FUNCTIONS USED IN THE BIOGEOCHEMICAL MODEL

Inputs from the 3D hydrodynamic model:
Temperature: °C, of water for each layer of the water column and above the sediment.
Salinity: PSU, of water for each layer of the water column
h= layer thickness, in meter
K_z = diffusivities, in $m^2.s^{-1}$
τ = bottom shear stress, in N.m-^{2}
The pycnocline depth, so the number of mixed and pycno layers are obtained from the maximal differences in density, using temperature and salinity inputs.

Inputs from the PP model:
PP: in mg C/m^2/day integrated on the mixed layers, coming from remote sensing data

Parameters, constants:
ζ = fraction of refractory carbon, ranging from 0.005 to 0.9
τcrit = 1 N/m^2 , critical shear stress at the bottom for POC deposition
K_{Z_SL}= sediment-water diffusivity of oxygen, ranging from 0.000864 to 0.0864 $m^2.d^{-1}$
K_{D_SL} = oxidation of POC in the sediment layer, ranging from 0.005 to 0.00005 day^{-1}
hbl = 0.2 m first estimation of the bottom layer thickness
hsl= 1.0 m thickness of the sediment layer, only used for the calculation of POC_sl_t0
V = net sinking or particles settling velocity, ranging from 0.5 to 5 $m.d^{-1}$
Ksed= $\frac{V}{h}$ in s^{-1} settling/sinking rate specifically calculated for each layer including the bottom layer
K_{BOD} = 0.5 mg O_2/l half saturation constant for oxygen limitation in oxidation of carbon
Θ_D^{T-20} = 1.047^{T-20} constant temperature rate (referred to 20°C), for oxidation of carbon in the water column
Θ_{DS}^{T-20} =1.08^{T-20} constant temperature rate for oxidation of carbon, in the sediment
Θ_R^{T-20} = 1.047^{T-20} constant temperature rate for respiration of the phytoplankton and all organisms on relation with primary production of oxygen
K_D = oxidation rate of POC in the water column, ranging from 0.003 to 1.0 day^{-1}
Oxy-sat id the oxygen concentration at saturation in water mg/l or g/m^{-3}, calculated on the basis of Weiss equations

$K_2c(T)$ is the reareration rate coefficient at ambient temperature, in day^{-1}
Kr is the global respiration rate of algae and other organisms, subtracted on the daily oxygen production, in day^{-1}
Kphotos is the photosynthetic conversion rate of primary producers from carbon to oxygen, in day^{-1}

Variables:

POC: Particulate Organic Carbon concentration, in mg C/ m^3
DO: Dissolved Oxygen concentration, in gO_2/m^3
DO_{ML}: index for DO concentration in the mixed layer, layers above the pycnocline
DO_{PL}: index for DO concentration pycno layers, below the pycnocline obtained from the calculation of maximum differences in densities between following layers; from Temperature and Salinity inputs.
DO_{BL}: index for DO concentration in the bottom layer, last layer above the sediment
DO_{SL}: index for DO concentration in the sediment layer
The state variables DO and POC are calculated for each box, from the surface to the sediment layers.

3.4 MODEL EQUATIONS OF OXYGEN/CARBON CYCLES IN COASTAL WATERS (PELAGIC/BENTHIC COUPLED MODEL)

This model is a deterministic and dynamic 1D biogeochemical model describing the general evolution of POC Particulate Organic Carbon and Dissolved Oxygen DO concentrations and flux in the water column and the sediment. POC is computed first and used afterwards for DO calculation.

POC variables

For all mixed layers

$$\text{sms(POC)}=\frac{\partial}{\partial t} POCml = POCmlt+1 = \text{PPt}+1 + POCml_{x-1}t+1 \times Ksed \times dt$$
$$- K_D \Theta_D^{T-20} \times POCml_x t+1 \times dt - POCml_x t+1 \times Ksed \times dt + POCml_x t$$

The primary production is calculated on the mixed layer and divided equally between each layer above the pycnocline as inputs for POC and DO.

For all pycnocline layers

$$\frac{\partial}{\partial t} POC_{pycno} x = POC_{pycno} xt+1 = POCpycno_{x-1}t+1 \times Ksed \times dt$$
$$- \left(K_D \Theta_D^{T-20} \times POCpycno_X t+1\right) \times dt - \quad POCpycno_X t+1 \times Ksed \times dt + \text{POCpycno}_X\ \text{t}$$

For the bottom layer

$$\frac{\partial}{\partial t} POC_{bl} = POC_{bl}t+1 = POCpycnq_t+1 \times Ksed \times dt$$

$$- K_D \Theta_D^{T-20} \times POCbl_{t+1}\left(1 - \left[V \times \left(1 - \frac{\tau}{\tau_{crit}}\right)\right]\right) \times dt \ + \text{POCbl t}$$

Sediment box

$$\text{sms(POC)} = \frac{\partial}{\partial t} POCsl = \left(POCbl\right)\left[V \times \left(1 - \frac{\tau}{\tau_{crit}}\right)\right] \times dt$$

$$- K_{D\_SL} \Theta_S^{T-20} \times POCsl(1-\zeta) \times dt + POC_{sl}t$$

$$POCsl_{t+1} = \ \left(POCbl\right)_{t+1} dt \ \left[V \times \left(1 - \frac{\tau}{\tau_{crit}}\right)\right] - K_{D\_SL} \Theta_S^{T-20} \times POCsl_{t+1}(1-\zeta) \times dt + POC_{sl}t$$

$$\text{sms(DO)} = \ \frac{\partial}{\partial t} DOs = \ \left(K_{D\_SL} \Theta_{DS}^{T-20}\right) POCsl$$

$$DOsl_{\ t+1} = K_{D\_SL} \Theta_{DS}^{T-20} (1-\zeta) POCsl_{\ t+1} dt \ + \ DOsl_{\ t}$$

$$\text{SOD}_{t+1} = \frac{K_{ZSL}}{Hbl} \times \left(\frac{DOsl}{Hsl} t+1\right)$$

SOD or Sediment Oxygen Demand is in $gO_2/m^3/s$

Oxygen variables

For all mixed layers

$$\text{sms(DO)} = \frac{\partial}{\partial t} DO_{ML} = DO_{ML}t+1 = K_2\left(DOml_{t+1} - Oxy - sat_{t+1}\right)dt$$

$$+ PPt+1 \times \frac{32}{12} \times Kphotos \times dt - PPt+1 \times Kr\Theta_R^{T-20} \times dt \ - \left(K_D\right)\Theta_D^{T-20}$$

$$\times \left(\frac{DO_{ML}}{DO_{ML} + K_{BOD}}\right) \times POC_{ml}t+1 \times dt \ + \ \frac{\partial}{\partial z}\left(Kz \frac{\partial}{\partial z} DO_{ML}t+1\right) \times dt + DO_{ML}t$$

Normally models consider reaeration at the top layer only; this model applies a reaeration model to all layers in the mixed layer with the reaeration coefficient as a function of wind and current speed. This implicitly assumed the mixed layer is well mixed. This assumption is necessary in this model because no advection is considered.

Oxygen is the transported to the lower layers via diffusion-in reality some advection would also occur but this is not considered in this 1-D model. The concentration of oxygen is calculated for each layer of the mixed layer using the diffusivity equation, as for the pycnocline layers. Primary production is the main source of oxgen production and converted from mg C/ m^3 in gO_2/m^3, using the carbon to oxygen ratio of $\frac{32}{12}$ and the photosynthetic and respiration rates.

For all pycnocline layers

As for the POC pycno, the DO is calculated within each layer of the pycno and mixed layers

$$\text{sms(DO)}=\frac{\partial}{\partial t} DOpycno_n = DOpycno_n t+1 = \frac{\partial}{\partial z}\left(Kz \frac{\partial}{\partial z} DOpycno_n t+1 \right) \times dt -$$

$$\left(K_D\right) \Theta_D^{T-20} \times \left(\frac{DOpycno_{\ n}}{DOpycno_{\ n} + K_{BOD}} \right) \times POCpycno_{\ n} t+1 \times dt \ + \ DOpycno_n t$$

The same diffusion equation is applied for each layer below the pycnocline with input and output regulated by the general vertical diffusion equation between the above and below layer (cf. GETM model, Burchard & Bolding, 2002). This differential equation parameterizes the vertical diffusion for each layer of a water column within a physical model as a transport equation. While applying this discrete differential transport equation, for the vertical dimension, we used as prescribed, the second-order Crank-Nicholson time scheme for the resolution of these equations. Then, these linear equations corresponding to each layer are solved simultaneously, using a tri-diagonal matrix and the simplified Gaussian elimination (Samarskij, 1984).

For the bottom layer

$$\text{sms (DO)} = \frac{\partial}{\partial t} DObl = \frac{\partial}{\partial z}\left(Kz \frac{\partial}{\partial z} DObl \right) \times dt - \left(K_D\right) \Theta_D^{T-20} \times \left(\frac{DObl}{DObl + K_{BOD}} \right) \times POC -$$

$$SOD \times dt$$

$$DObl_{t+1} = \frac{\partial}{\partial z}\left(Kz \frac{\partial}{\partial z} DObl_{t+1} \right) \times dt - \left(K_D\right) \Theta_D^{T-20} \times \left(\frac{DObl_{t+1}}{DObl_{t+1} + K_{BOD}} \right) \times POC_{t+1} \times dt -$$

$$SOD_{t+1} dt + \ DObl_t$$

These equations have been applied including in Kz not only the turbulent diffusion, but also the molecular diffusivity, as a lower limit for in oxygen transport.

Initial conditions

All physical variables coming from GETM and remote sensing data are yearly and spatially specific to the site chosen. Therefore, we consider them as forcing functions valid as initial conditions, whereas for the biogeochemical model, some equations are specifically adapted, to settle the initial conditions.

POCml = PP
POC sl= POC_sl_t0
$POC_{bl} = 0$
$POC_{pycno} = 0$
$DO_{ML} = DO_{ML}t0$ coming from in situ measurements (last measurement average for the box before starting of the model run)
$DOpycno = DO_{pycno}t0$
$DObl = DO_{bl}t0$

The DO concentrations are calculated for all corresponding layer of mixed, pycnocline and bottom layers, except the sediment layer.

DOsl= $\left(K_{D\_S}\Theta_{DS}^{T-20}\right)POCsl \times dt$

$$\text{SOD} = \frac{Kz\_sl}{Hbl} \times \frac{DOsl}{Hsl}$$

$$DObl = \left(DO_{bl}t0 - SOD\right) \times dt$$

IV- RESULTS AND DISCUSSION

4.1 ONE-YEAR RUN OF THE MODEL FOR A FIRST-GUESS PARAMETERS VALUES

The values chosen for the parameters: rates and constants are taken from the literature, or in-situ measurements, either first-guess for the Baltic Sea (table 1). The time-step chosen is of 20 minutes to consider the continuity for calculation within each layer.

Table 1: Optimal values for the Belt sea station and the first-guess model run

PARAMETERS	Values	Units
h	0.97	m
Hbl	0.2	m
Hsl	1.0	m
dt	1200	s
Kphotos	0.0000115	s^{-1}
Kd_sl	0.000000058	s^{-1}
Kz_sl	0.0000001	s^{-1}
ζ	0.05	[-]
Kbod	0.5	[-]
Θ_{D}^{T-20}	$1.047^{(T-20)}$	[-]
Θ_{DS}^{T-20}	1.08^{T-20}	[-]
Θ_{R}^{T-20}	1.047^{T-20}	[-]
Ksed	0.0000596	s^{-1}
Θ_{R}^{T-20}	1.047^{T-20}	[-]
τcrit	1 .0	N/m2
K_2	From winds, Temp, depth	s^{-1}
K_D	0.00000175	s^{-1}
Kr	0.00000175	s^{-1}

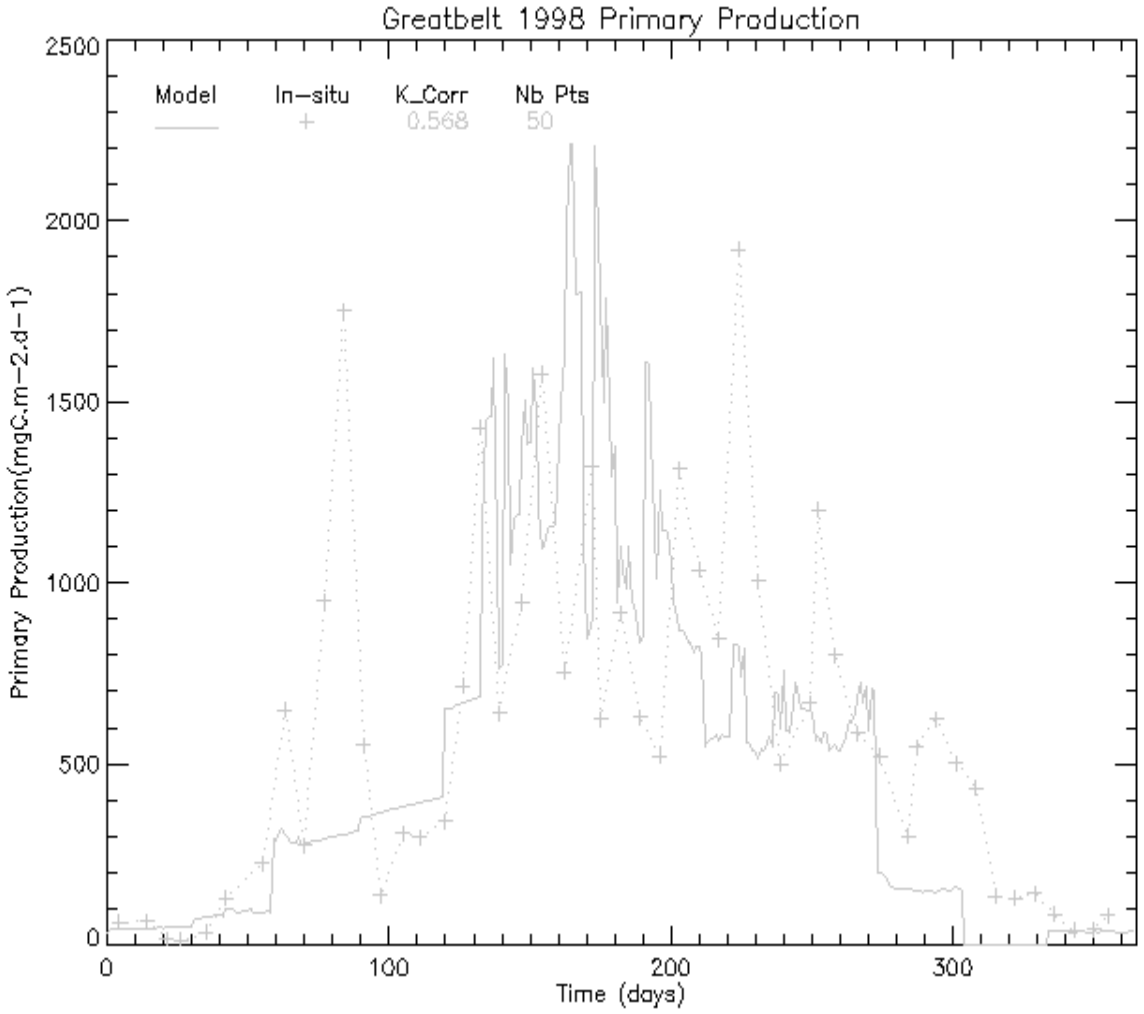

Figure 4: Temporal distribution of primary production with field measurements (straight line) and satellite data (dotted line) plots, for comparison.

The algorithm or model of PP calculation applied showed a good recovery of annual PP. For primary production, the matching of PP remote sensing/field data is good from late spring to autumn, with a good recovering of blooms or peaks for PP from late spring to autumn. Whereas winter and beginning of spring are not well covered, with an underestimation of blooms in winter/spring between satellite and in situ data (high level of cloudiness), the general agreement obtained between means satellite and in situ data is significant ($r^2 = 0.58$) and indicate a good recovery and of remote sensing data using this algorithm. By the way, the development of a more accurate algorithm for coastal or land-influenced areas (Jassby *et al.,* 2002) and its validation is still an ongoing work (Bouman *et al.,* a,b, 2000).

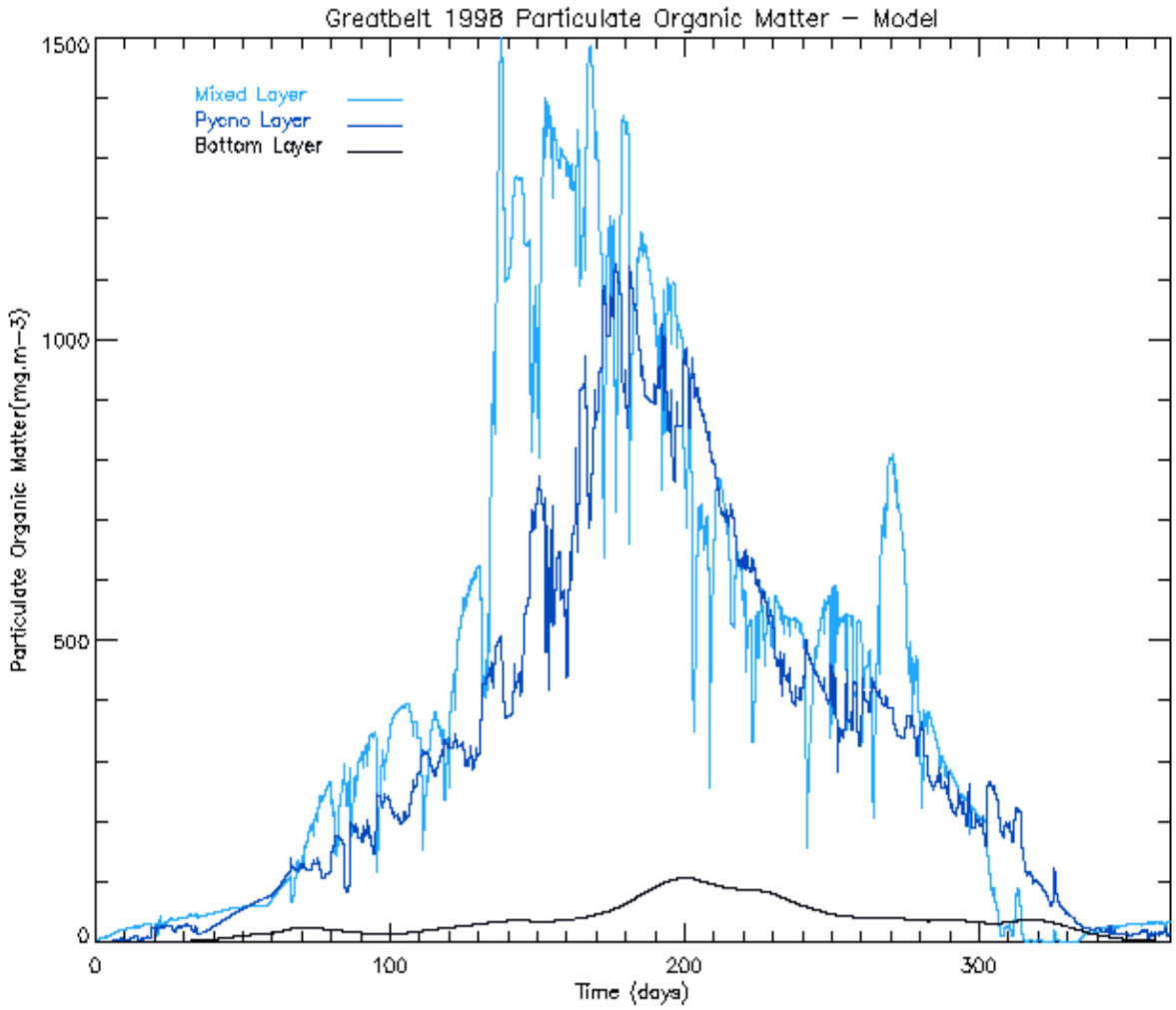

Figure 5: Temporal distribution of the different POC concentrations in each layer of the model, except the sediment layer (fig.8), for 1998 run (in Julian days). The blue scale from light to dark blue corresponds to the depth from the surface to the bottom. Mixed layers are in light blue, pycnocline layers are in dark blue, where the bottom layer is almost black.

The settling or accumulation through the water column is visible but buffered in these averaged layers, where the settling carbon is degraded gradually from surface to the bottom layer. The link with primary production as input for POC shows the same seasonal variation and trends, (see fig.4) with POC input or POC production with delays between PP peaks in the mixed layer and POC-in corresponding peaks in the pycno and bottom layers.

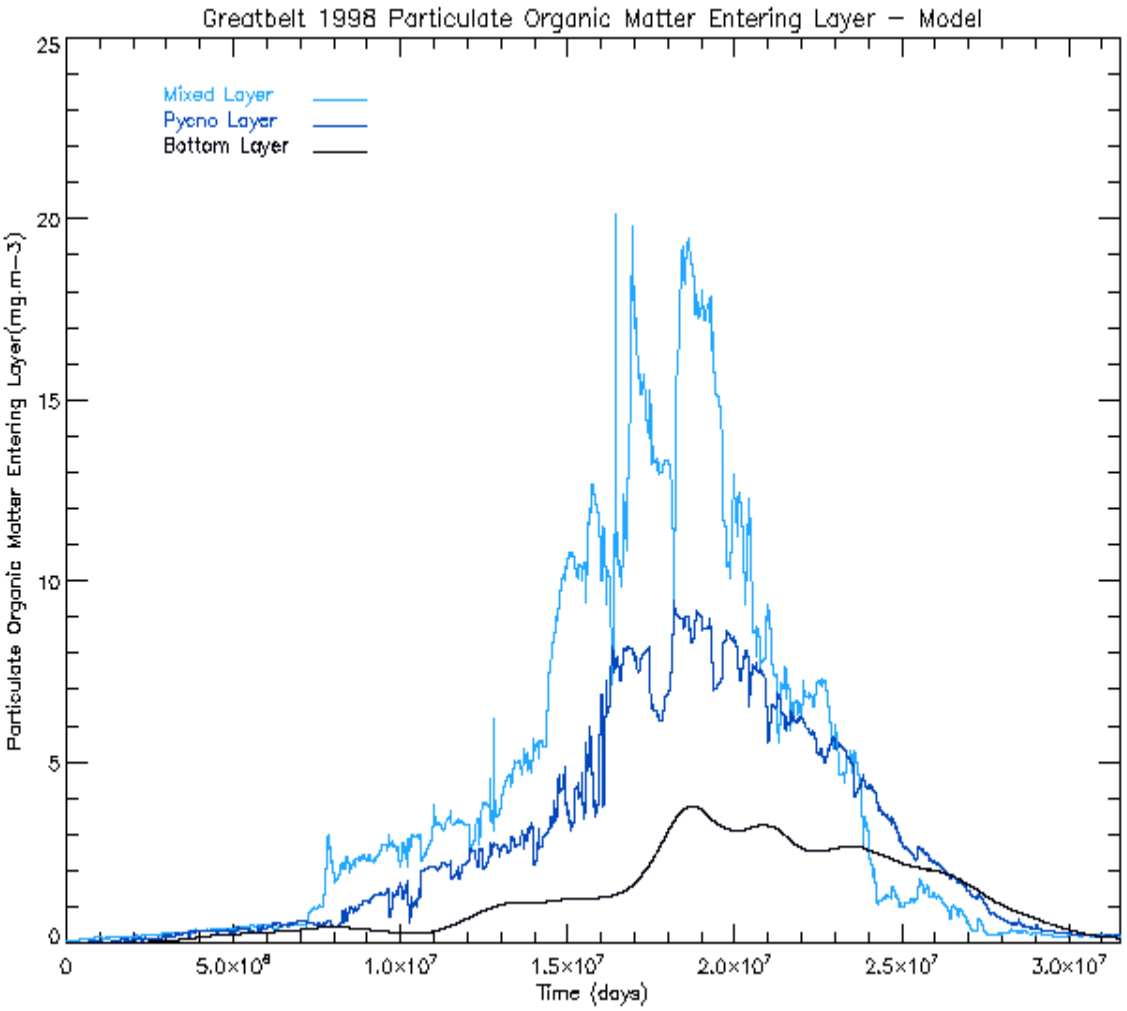

Figure 6: Temporal distribution of the different POC-in concentrations or input of Particulate Organic Carbon in each layer of the model, for 1998 run (in Julian days). The same scale as for fig.5 applies.

This variable corresponds to the PP and settling carbon arriving from the above layers.

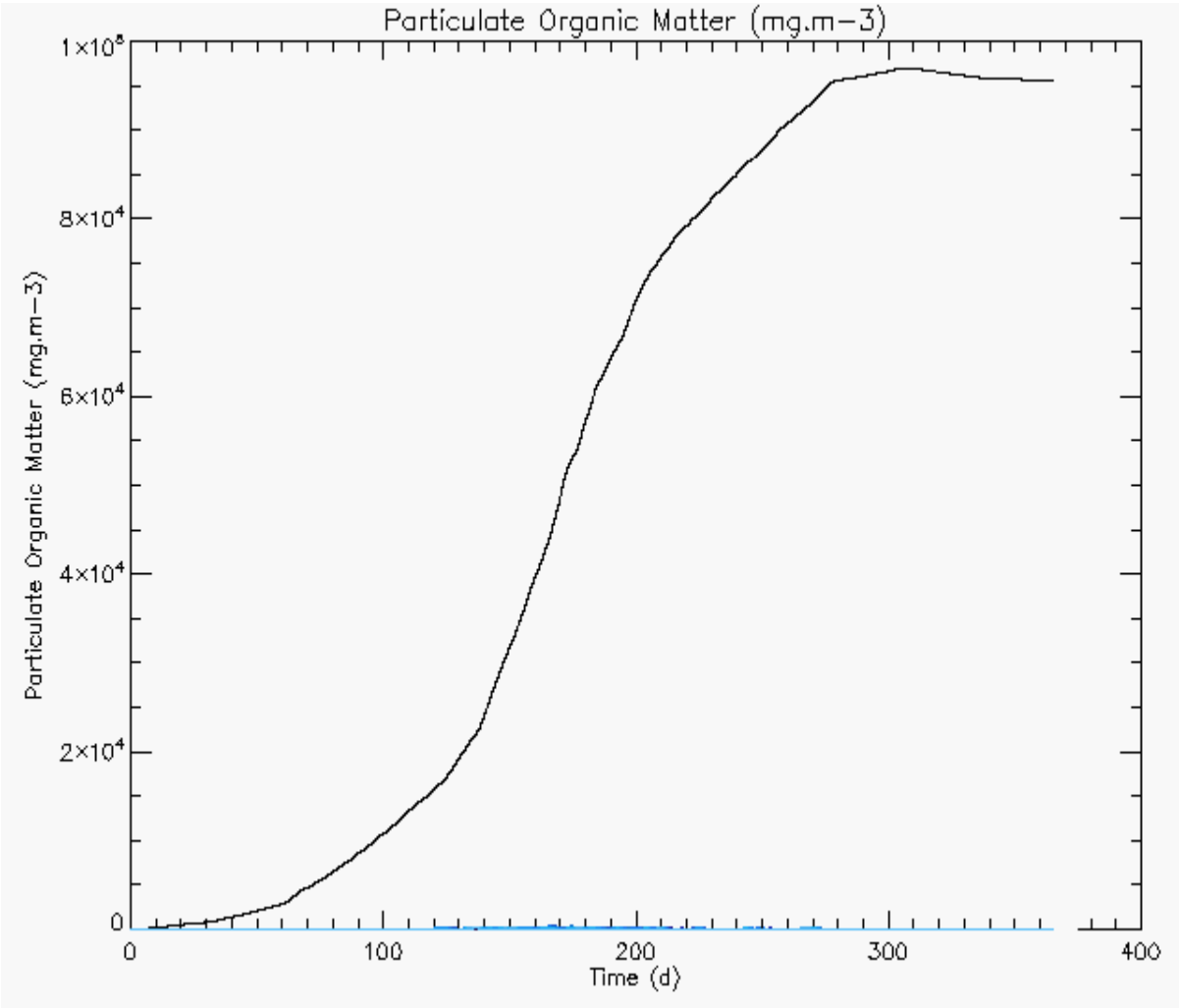

Figure 7: Temporal distribution of different POC-in concentrations for all layers, including the sediment layer (black line). The sediment layer has the highest amounts of carbon inputs or production due to accumulation and sedimentation combined effects and a low oxidation rate. Therefore, for the other linked POC variables their respective sediment quantities or concentrations of carbon are always higher than in the other layer.

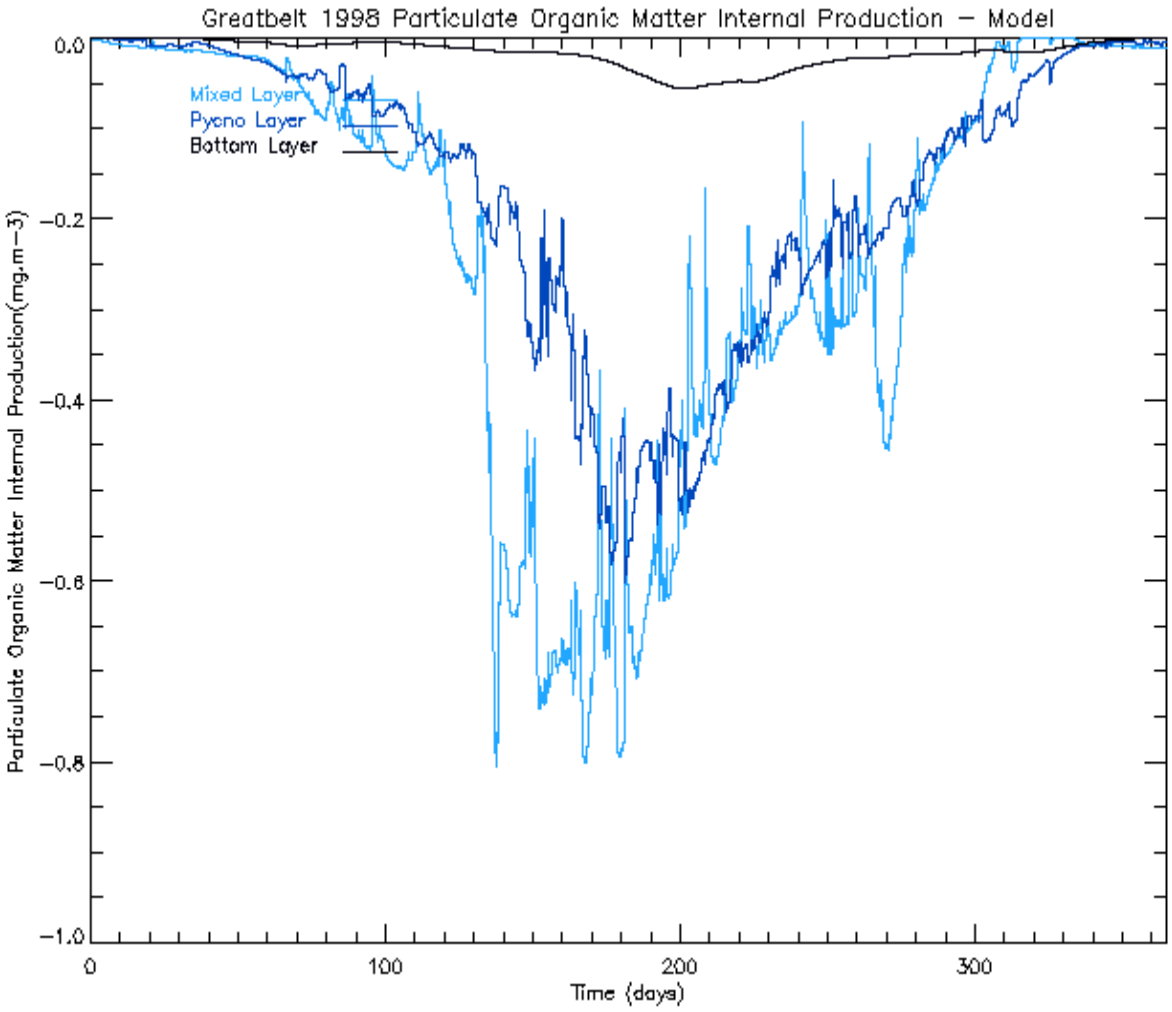

Figure 8: Temporal distribution of the different POC-intern concentrations or degradation of Particulate Organic Carbon in each layer of the model, for 1998 run (in Julian days). The same scale as for fig.5 applies.

This variable is temperature dependant and corresponds only to consumption and oxidation processes in water and sediment.

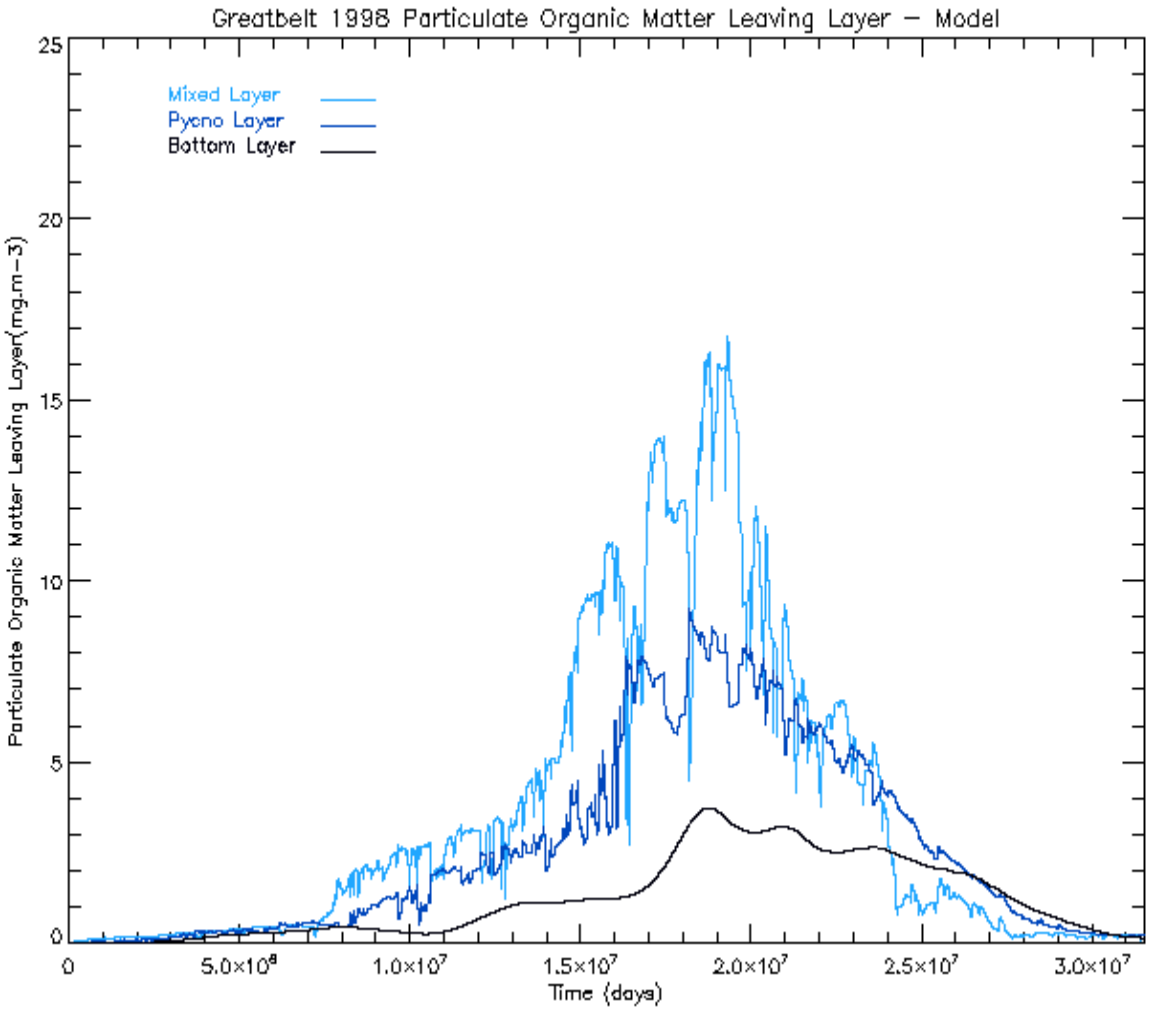

Figure 9: Temporal distribution of the different POC-out concentrations or leaving Particulate Organic Carbon for each layer of the model, for 1998 run (in Julian days). The same scale as for fig.5 applies.

This variable corresponds only to settling POC from one layer to another one. The highest absolute amounts of settling carbon are observed in the first pycnocline layers, where the maximum amount of POC not yet degraded is arriving, following each bloom or carbon production, seen in the mixed layer. The averaged layers show the relative and regular degradation between mixed pycno then bottom layers.

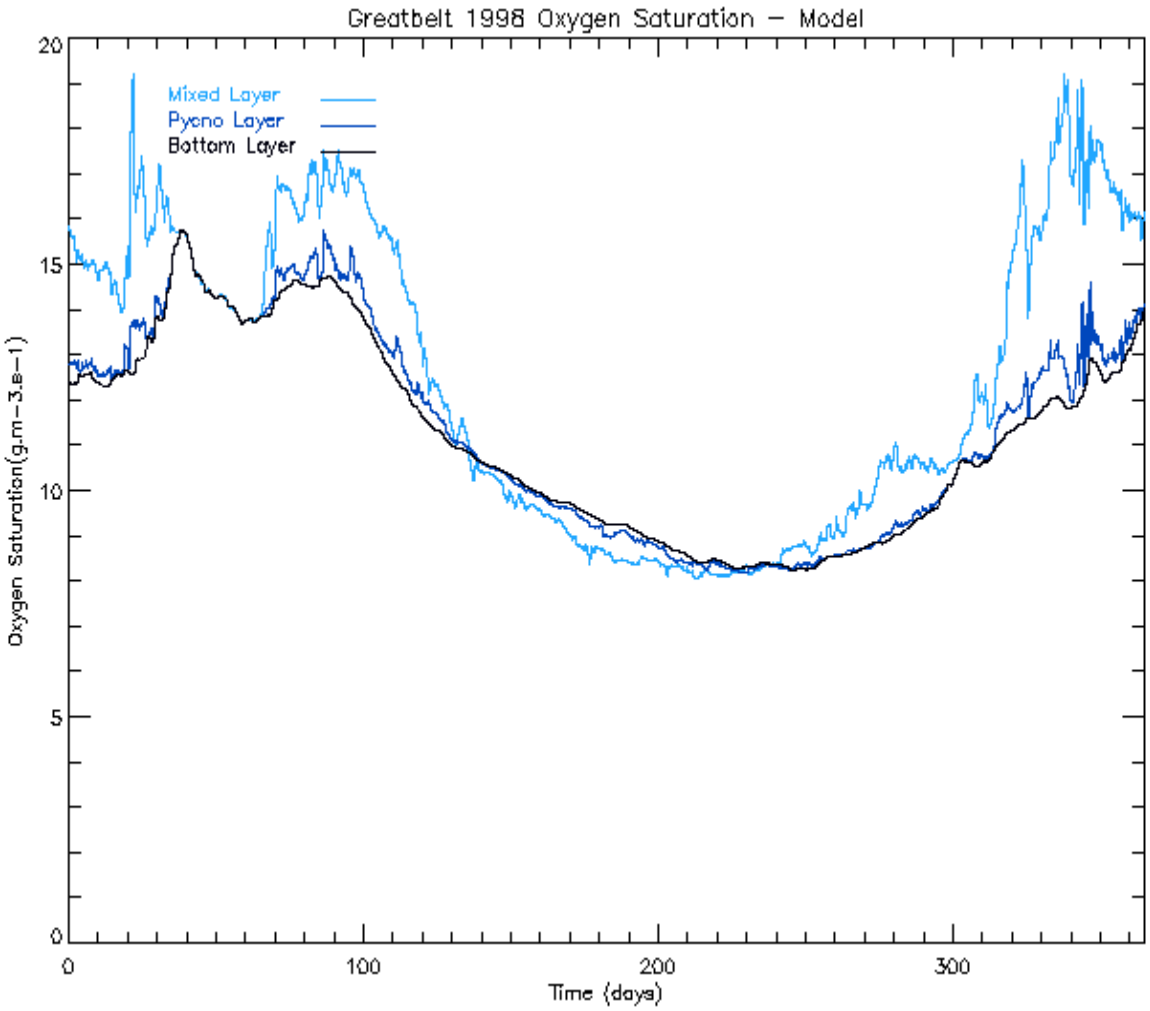

Figure 10: Temporal distribution of oxygen saturations during 1998, for Great Belt station in the different averages layers. The same scale as for fig.5 applies.

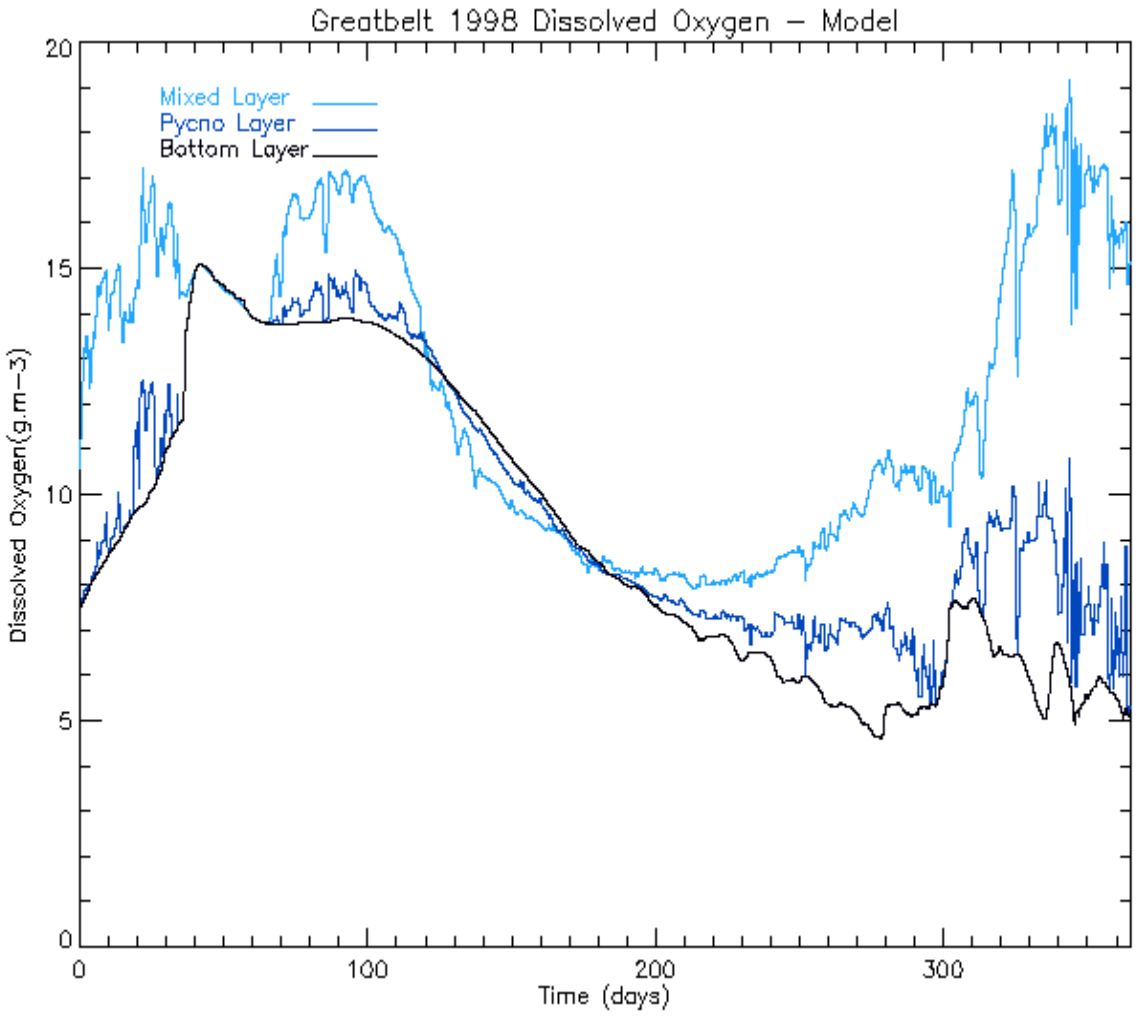

Figure 11: Temporal distribution of the DO concentrations for the averaged layers of the model, for 1998 run (in Julian days). The same scale as for fig.5 applies.

This balance for dissolved oxygen concentrations is mainly influenced by the physical factors, then by the accumulation or consumption of oxygen, following the spring and summer peaks in POC production and oxidation in the bottom layers. During spring, a first inversion is observed between deep and surface layers, where warmer surface layer showed less concentration of oxygen than the deepest and coldest layer: bottom layer (cf. fig.10). The second inversion is observed after 180 days, so at the beginning of summer. At that time, mixed layers represent the more oxygenated part of the water column due to primary production and reaeration, whereas the bottom layer decreased to its minimum, close to hypoxic concentrations, due to sediment sinks or carbon oxidation. The minimum concentrations of DO is estimated at the end of the summer around 250-280 days, when the different and following blooms have sedimented, consumed all oxygen benthic stocks and increased the consumption of oxygen, and hence all buffering possibility of benthic layers. After this minimum oxygen concentrations, DO tend to be dominated again by the physical forcing functions i.e: temperature, salinity and winds exchanges for the entire water column.

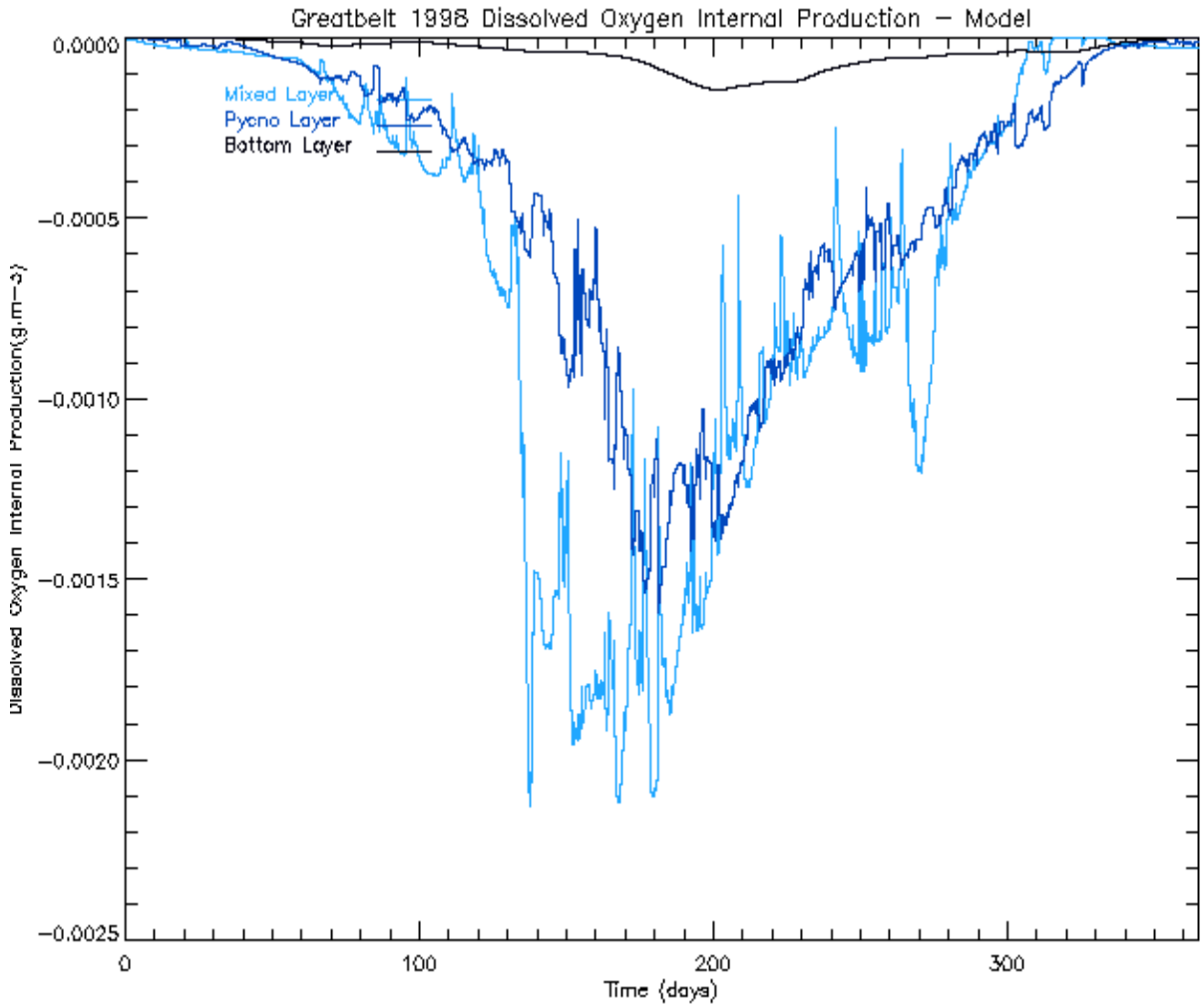

Figure 12: Temporal distribution of the DO-intern concentrations for each averaged layer of the model, for 1998 run (in Julian days). Same scale as for other figures applies.

These concentrations or fluxes correspond to the oxidation of POC in each layer. The highest consumption of oxygen is those of the sediment layer, where the carbon concentration is the highest (cf. fig.7).

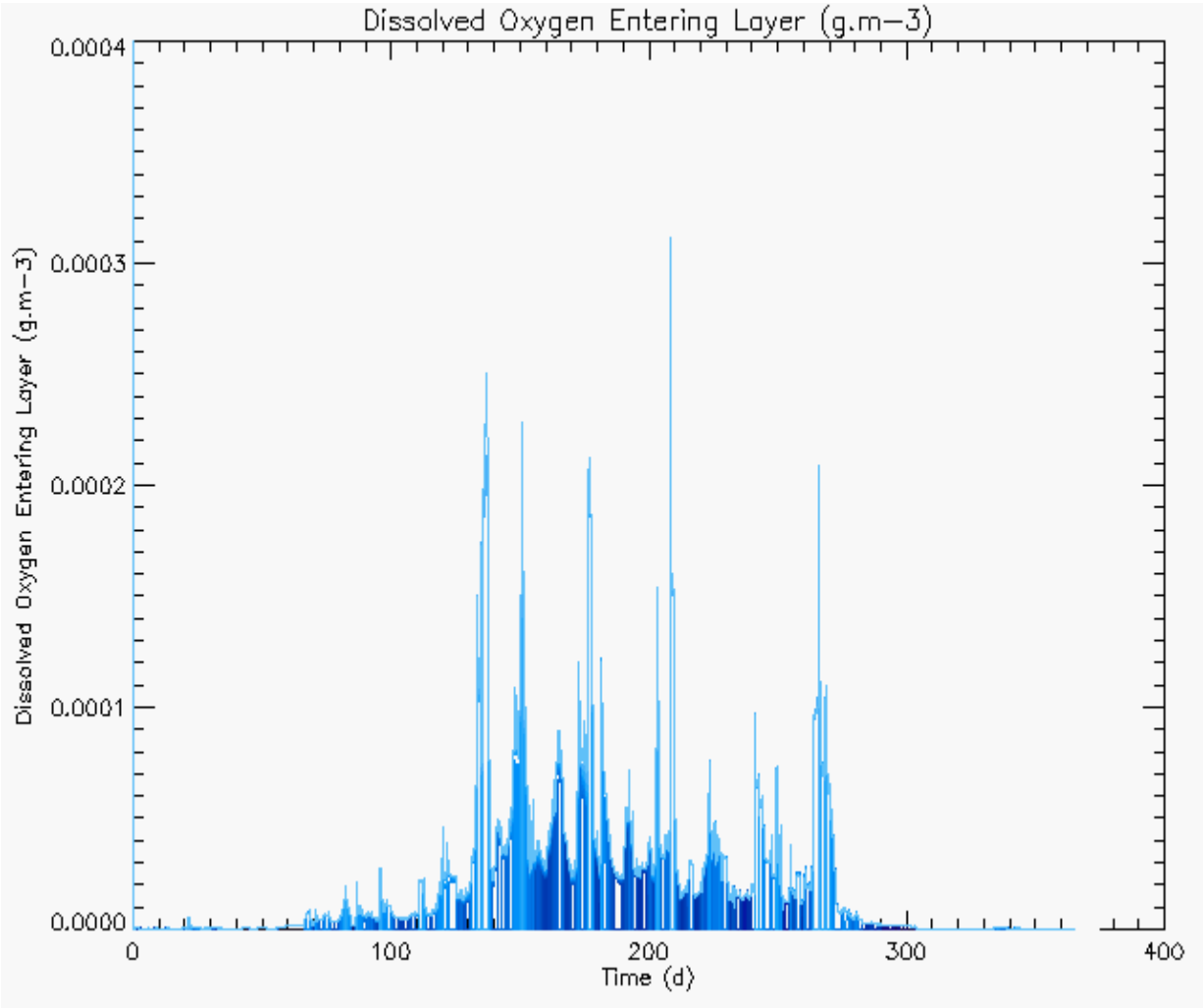

Figure 13: Temporal distribution of the DO-in concentrations for each layer of the model, for 1998 run (in Julian days). DO-in is only quantified in the mixed layer, with light blue for surface layers and darkest blue for the deeper ones.

Oxygen production volumes are quantified in the mixed layer, where there is a primary production, using photosynthetic conversion rate from carbon to oxygen and incorporation of the respiration rate of various planktonic organisms. This input of oxygen is linked to phytoplankton blooms intensities and distribution on the mixed layer thickness.

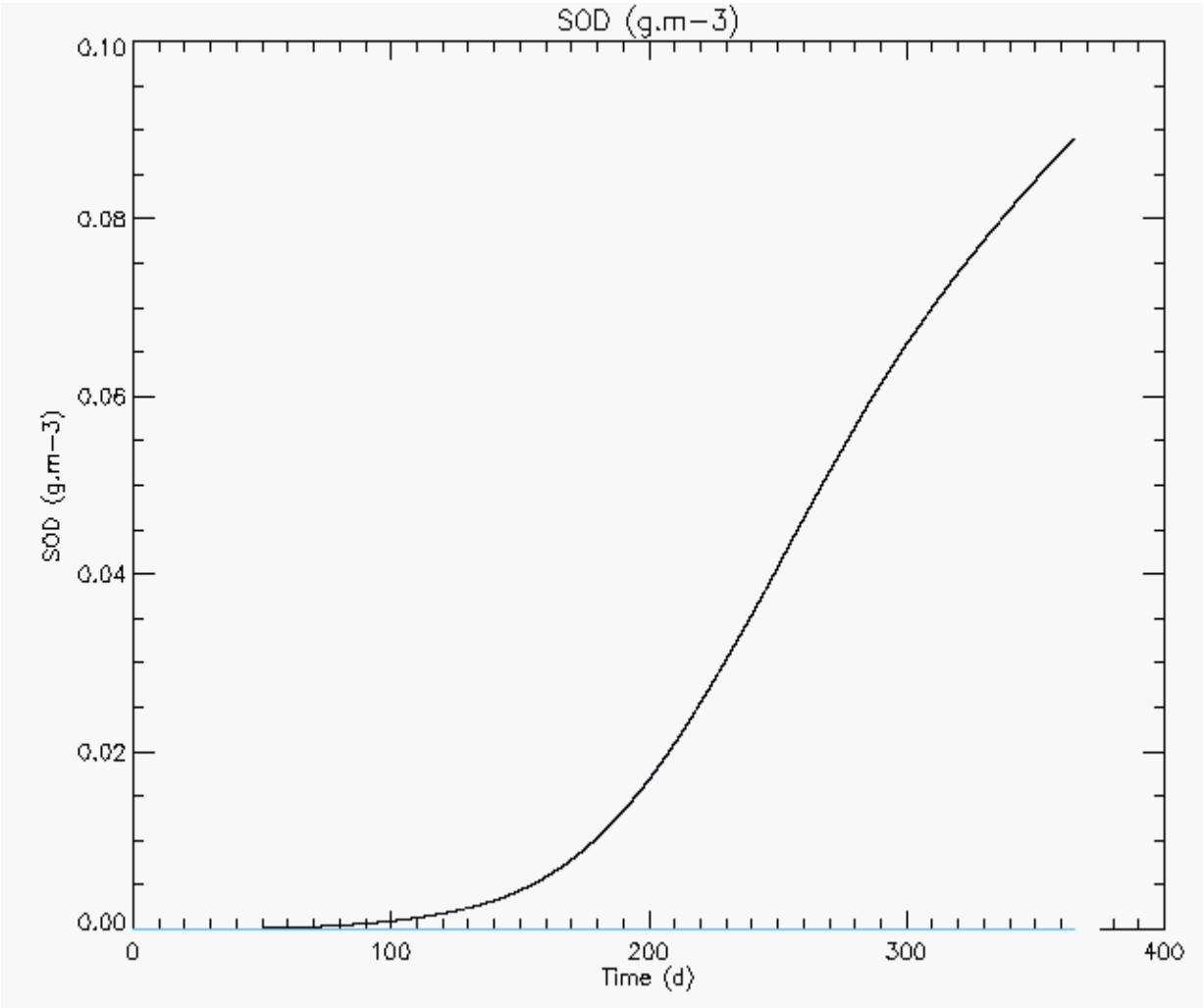

Figure 14: Temporal distribution of the SOD or Sediment Oxygen Demand for Great Belt station, 1998 run (in Julian days).

This SOD or Sediment Oxygen Demand corresponds to the sediment need of oxygen and variation of the water-sediment diffusion coefficient, temperature dependant.
For all other water layers, leaving or entering oxygen flux is quantified through the vertical diffusion equation, using the diffusivities for above and bottom layers.

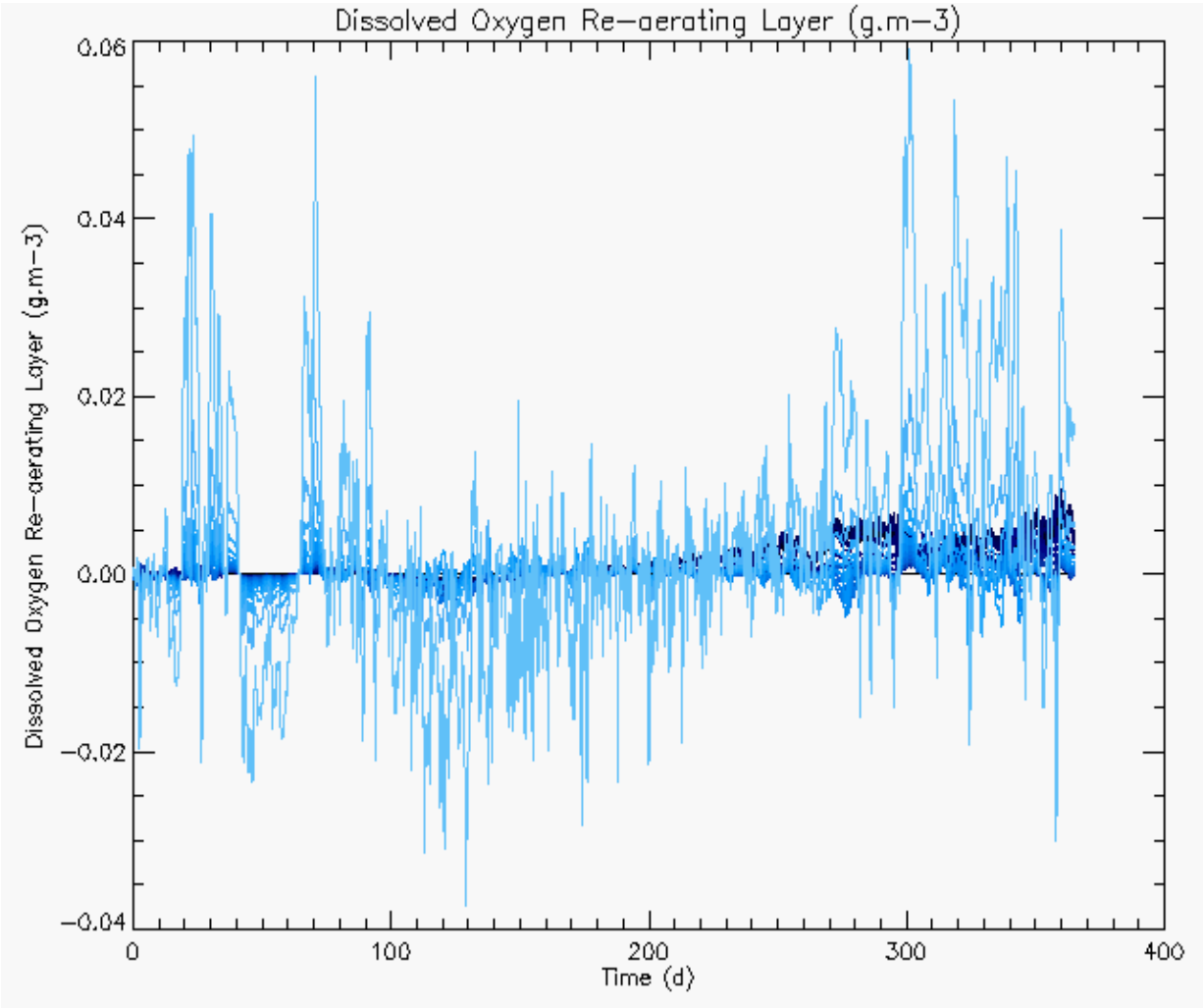

Figure 15: Temporal distribution of the DO-reaer concentrations for each layer of the model, for 1998 run (in Julian days).

The quantified concentrations of oxygen due to wind stress or air/water exchange are processed for the different layers, depending on the depth of each layer and the strength of the wind. When negative, the flux of oxygen is transmitted from water column to air, and inversely if positive, oxygen is entering in the surface layers. This process is buffering the oxygen consumption/production processes in water, and overcomes them especially during winter and autumn seasons, following the wind stress fluctuations. For instance, highest quantities of DO exchange due to reaeration are visible between 20 and 40 days, then after 300 days up to the end of the year run.

4.2 SENSITIVITY ANALYSIS

1) Parameters and ranges tested for the sensitivity of the model

For the sensitivity analysis all physical variables as the primary production inputs are prescribed variables. The diffusivity and reaeration rate Kz and K2 were also considered as prescribed because they are calculated using prescribed variables and are already validated, as for the different temperature-dependant constants: Θ_R^{T-20}, Θ_D^{T-20} or Θ_{DSL}^{T-20}.

Finally, two global sensitivity analyses of the model parameters have been performed varying over the range found in the literature for each particular parameter (table 2). The first analysis was computed with 3 different sets of values for the parameters: the first-guess optimal values, the maximum and minimum values of the parameter intervals. The second following the first guess run and some further analyses on a new optimal set of values (table 6-7). These calculations were computed using the formula of Friedrichs (2001) with an IDL program, in order to assess the correlation between parameters and the model variables, as to test the stability and possible local maxima or minima of the model parameters (Jorgensen & Bendoricchio, 2002).

Table 2: Parameters and ranges of values (daily rates)

PARAMETERS	Optimal values	Range of values step	Minimum step	Maximum step
Kz_sl	0.00864	0.00864	0.000864	0.0864
Kd_sl	0.005	0.0025	0.001	0.05
ζ	0.05	0.01	0.001	0.05
POC_sl_t0	172.6	4.0	2.0	170.0
Kr	0.15	0.01	0.01	0.15
Kphotos	1.0	0.25	0.25	2.0
Kd	0.15	0.05	0.05	1.0
V	5.0	0.5	0.5	10.0

For the model sensitivity results, the sensitivities up to 10^{-6} have been considered. Below this number, the calculation was neglected considering the error computing and so a nul result written.

2) First Sensitivity analysis : for parameter optimal values

The symbol X is used when no change is observed for the different C_X .

All calculations were performed independently, for each state variable and within them for each box, allowing an estimation of parameters independence and influence on each box of the variables. For instance: Sml DO is the sensitivity index for DO in the mixed layer and Sbl POC would be the sensitivity index for POC in the bottom layer.

During this first analysis, we tested small values for parameter zeta. Consequently, the parameter zeta used for the buried or non degradable fraction of the carbon, was found to be independent or uncorrelated to any variables and parameters considered. Local maxima were found for Kd for the values 0,3 to 0,4 and for variables DO pl and DO bl where the sensitivity value was two times higher, but still the values are weak.

Table 3: Model sensitivity analysis to parameter variations, first set of optimal values

Parameters/ Variables	S ml DO	S pl DO	S bl DO	S sl DO	S ml POC	S pl POC	S bl POC	S sl POC
Kz_sl	-0.000002 -0.002	-0.0001 -0.1	-0.0002 -0.21	X	X	X	X	X
Kd_sl	0.000	0.000	0.000	1.0	X	X	X	-0.042 -2.669
POC_sl_t0	0.000	0.000	0.000	1.0	X	X	X	0.0010 0.0025
ζ	X	X	X	X	X	X	X	X
Kd	-0.0012 -0.012	-0.01 -0.0164	-0.012 -0.033	X	-0.022 -0.464	-0.088 -3.124	-0.136 -12.023	-0.132 -10.737
Kr	-0.0000016 -0.00002	-0.0 -0.000004	0.0	X	X	X	X	X
Kphotos	0.000001 0.0002	0.00001 0.00033	0.0	X	X	X	X	X
V	0.0015 0.0040	0.015 0.030	0.020 0.038	X	-0.093 -2.239	-0.042 -1.736	0.187 -4.731	4.20 0.43

3) Sensitivity analysis: For parameter minimal values

Table 4: Model sensitivity analysis to parameter variations, minimal values chosen as optimal values

Parameters/ Variables	S ml DO	S pl DO	S bl DO	S sl DO	S ml POC	S pl POC	S bl POC	S sl POC
Kz_sl	-0.0000012 -0.0001	-0.000075 -0.0069	-0.00013 -0.0122	X	X	X	X	X
Kd_sl	-0.000 -0.0000012	-0.000023 -0.000092	-0.000039 -0.000166	1.0	X	X	X	-0.1809 -3.0594
POC_sl_t0	X	-0.000 -0.000	-0.000 -0.000	1.0	X	X	X	0.00093 0.00957
ζ	X	X	X	X	X	X	X	X
Kd	-0.0083 -0.0083	0.01906 0.0504	0.0396 0.0607	X	-0.500 -4.864	-2.109 -66.989	-5.35 -637.60	-4.445 -303.024
Kr	-0.000003 -0.000024	-0.000002 -0.000010	-0.0000015 -0.000005	X	X	X	X	X
Kphotos	0.000082 0.00033	0.000029 0.000117	0.000009 0.000039	X	X	X	X	X
V	0.00796 0.0105	0.01768 0.05412	0.00718 0.0561	X	-1.477 -17.655	-0.529 -8.329	0.109 -13.362	1.158 0.858

Local maxima were again found for Kd within the range of values of 0,25 to 0,4 but for variables DO ml and DO bl ; for which the sensitivity value was two times higher, than the sensitivity of range boundary values.

4) Sensitivity analysis : For parameter maximal values

Table 5: Model sensitivity analysis to parameter variations, maximal values of the range parameters chosen as optimal values

Parameters/ Variables	S ml DO	S pl DO	S bl DO	S sl DO	S ml POC	S pl POC	S bl POC	S sl POC
Kz_sl	-0.000012 -0.00114	-0.00116 -0.1180	-0.00212 -0.2389	X	X	X	X	X
Kd_sl	-0.000022 -0.000017	-0.00217 -0.01319	-0.00402 -0.02851	1.0	X	X	X	-0.01598 -0.8217
POC_sl_t0	-0.000 -0.00003	-0.000012 -0.000375	-0.000022 -0.000666	1.0	X	X	X	0.00018 0.0054
zeta	X	X	X	X	X	X	X	X
Kd	-0.0003 -0.0035	0.0102 0.1882	0.0296 0.4041	X	-0.0109 -0.2118	-0.031 -0.7709	-0.0407 -1.3262	-0.0399 -1.2638
Kr	-0.0000016 -0.0000250	-0.000 -0.000011	-0.000 -0.000006	X	X	X	X	X
Kphotos	0.000041 0.000288	0.000016 0.000117	0.000006 0.000048	X	X	X	X	X
V	0.00042 0.00523	-0.0079 -0.1697	-0.0132 -0.365	X	-0.0394 -0.903	0.1037 -0.301	0.4757 -1.5316	6.5963 1.4083

No local maxima were found for Kd, as we have tested the maximal value for this parameter and the others, while the settling velocity of V shows a local maxima for V = 1,0 to 1.5m/day for the DO variables between the pycno and sediment layers

5) Second sensitivity analysis

After a first calibration, we applied a second sensitivity analysis, to check the parameters influence and stability after modification. This additional step was compulsory due to improvements made in the parameterization of SOD and DO in the model.

Table 6: Optimal values chosen for the second sensitivity analysis (after a first calibration)

PARAMETERS	Optimal values	Range of values step	Minimum step	Maximum step
Kz_sl	0.000864	0.00864	0.000864	0.0864
Kd_sl	0.002	0.0025	0.001	0.05
ζ	0.5	0. 1	0.5	0.9
POC_sl_t0	2.0	4.0	2.0	170.0
Kr	0.15	0.01	0.01	0.15
Kphotos	1.0	0.25	0.25	2.0
Kd	0.15	0.05	0.05	1.0
V	5.0	0.5	0.5	10.0

SOD is parameterised using the relations between zeta, POC concentrations and oxidation rate of the sediment layer. This parameterisation and hence the effects of SOD will be very sensitive to the value of ζ which could approach a value of 1.0 for deeper waters.

In such cases *DOsl* and SOD would approach zero. A low range of ζ was used in the previous sensitivity analysis. We therefore tested a higher range of values be used in the second sensitivity analyses (e.g. 0.5-0.90), showing a real difference for Kz_sl and Kd_sl (see table 7).

Table 7: Model sensitivity analysis to parameter variations, following a calibration run new optimal values have been chosen for the sensitivity analysis and model run

Parameters/ Variables	S ml DO	S pl DO	S bl DO	S sl DO	S ml POC	S pl POC	S bl POC	S sl POC
Kz_sl	-0.74 -1.40	1.06 1.00	1.03 1.00	1.03 1.00	X	X	X	X
Kd_sl	-0.13 -1.03	1.20 0.99	1.09 0.98	1.09 0.98	X	X	X	X
POC_sl_t0	-0.000 -0.00003	- 0.000012 - 0.000375	-0.000022 -0.000666	1.0	X	X	X	0.00018 0.0054
ζ	X	X	X	X	X	X	X	X
Kd	-0.0003 -0.0035	-0.25 1.95	-0.18 3.66	-0.18 3.66	-0.026 -0.536	-0.25 1.95	-0.14 -13.33	-0.13 -11.76
Kr	- 0.0000011 - 0.0000016	-0.000 - 0.000018	-0.000 -0.000006	X	X	X	X	X
Kphotos	0.000026 0.000216	- 0.000013 - 0.000121	-0.000001 -0.000014	- 0.000001 - 0.000014	X	X	X	X
V	-0.0033 -0.021	-0.175 0.896	-0.297 0.644	-0.296 0.644	- 0.0394 -0.903	0.1037 -0.301	0.4757 - 1.5316	6.5963 1.4083

Local maxima were found for Kd, for DO in the pycno, benthic and sediment layers, for the range between 0,25 and 0,3 for Spl and between 0,45 and 0,5 for Sbl and Ssl. While the settling velocity of V shows a local maxima for V = 1,5 to 2,5 m/day for the DO variables between the pycno and sediment layers. Local maximum immediately following local minimum were also found for Kz_sl for the mixed layer only and DO variable, for Kz_sl = 0,0181 and 0,026. Globally Kz_sl and Kd_sl showed higher sensitivities, than in the previous analysis, due to zeta influences not visible directly in the sensitivity analysis and unconstrained of DO calculation in the sediment and bottom layers.

4.3 GENERAL TRENDS AND DISCUSSION FOR THE SENSITIVITY ANALYSIS

The different analysis highlight the robustness of the parameters and some specific areas to be attentive to, as the local maxima of Kd, when the optimal value is below 0,4 day $^{-1}$ (cf. fig.18) or the possible inversion of the variable sl POC if the sinking velocity chosen is of 1,0 or 2,0 m/day (cf. fig. 16).

These peculiarities exposed, the values of the sensitivities for Spoc and Sdox listed in table 2-4 and 7 are highly correlated to the oxidation rate and the sinking speed: V and Kd, for the different layers (fig.16 and fig.18). This analysis confirmed the relationship, between oxygen concentration in the sediment layer and amount of carbon in this layer for oxidation rate (see table 3-7). There is an inverse correlation between DO and POC variables for Kd

(fig.18, 19). Oxygen variables sensitivities are rather low compared to POC variables in the case of Kd and V, especially for the minimum or optimal values sensitivity analysis. They are proportionally correlated to their initial value as S_{plDO} and S_{blDO} S_{slDO} maximum values are found for maximal initial values, when used as reference values (fig. 16-17 and fig.18-19). Inversely, the sensitivity of POC variables to Kd is somehow higher, they are highly correlated and sensitive to the rising of these parameters. POC variables are also highly and strongly correlated to the sinking velocity as visible in fig.17, but with slightly lower values of the sensitivity. The lowest values of sensitivity were found for the upper boundary analysis (table 5), whereas with the minimal values or first set of optimal values, sensitivities are highest (table 3, 4). For Kd, the correlation or sensitivity increases with water depth, from the surface to the bottom layer. This parameter is directly influencing the carbon concentration in the water and hence the sediment. The sediment layer is also highly correlated with Kd but with slightly lower values than the bottom layer; as other parameters interact with the POC sediment layer dynamic (fig.20).

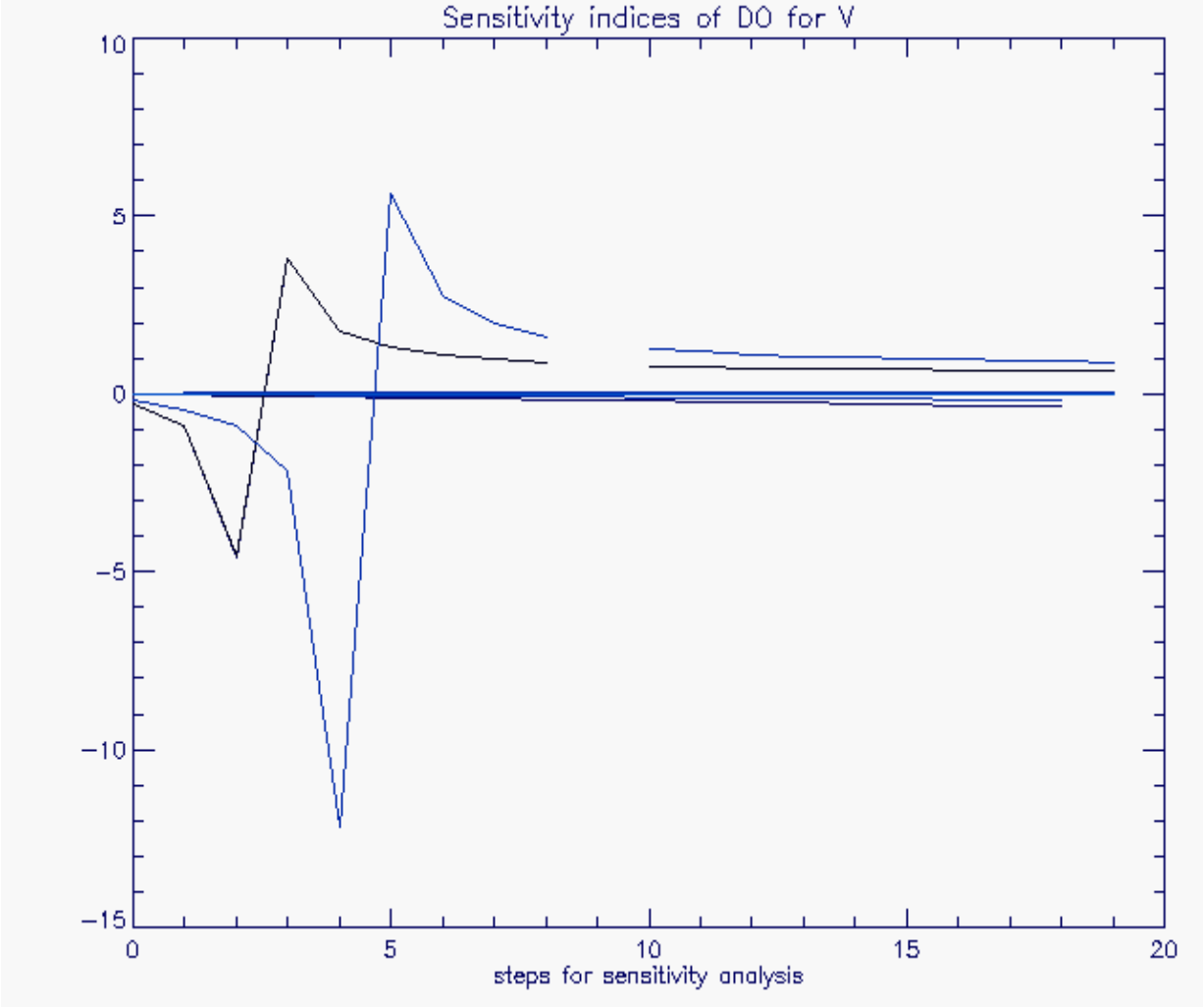

Figure 16: Plot of different sensitivity analysis for DO variables on the sinking velocity. Colour scale: Sml are drawn in light blue, Spl in blue, Sbl in dark blue, Ssl in black. (Lags in lines corresponds to optimal values ranges so no results in the corresponding sensitivity calculation)

Almost all S_{DO} sensitivities are plotted around 0 value, indicating a low sensitivity of DO to V whatever the layer or compartment is should be, as the initial value of sinking velocity (optimal, maximal, minimum). Maximal sensitivities are obtained for the bottom and sediment boxes, so the deepest ones in the second analysis, with local minimum of -5.0 and -12.0, immediately counterbalanced by maximum of 4.0 and 7.0 for values of V between 1.0 and 2.5, whereas all other compartments and sensitivity values indicate a low sensitivity of this parameter with DO.

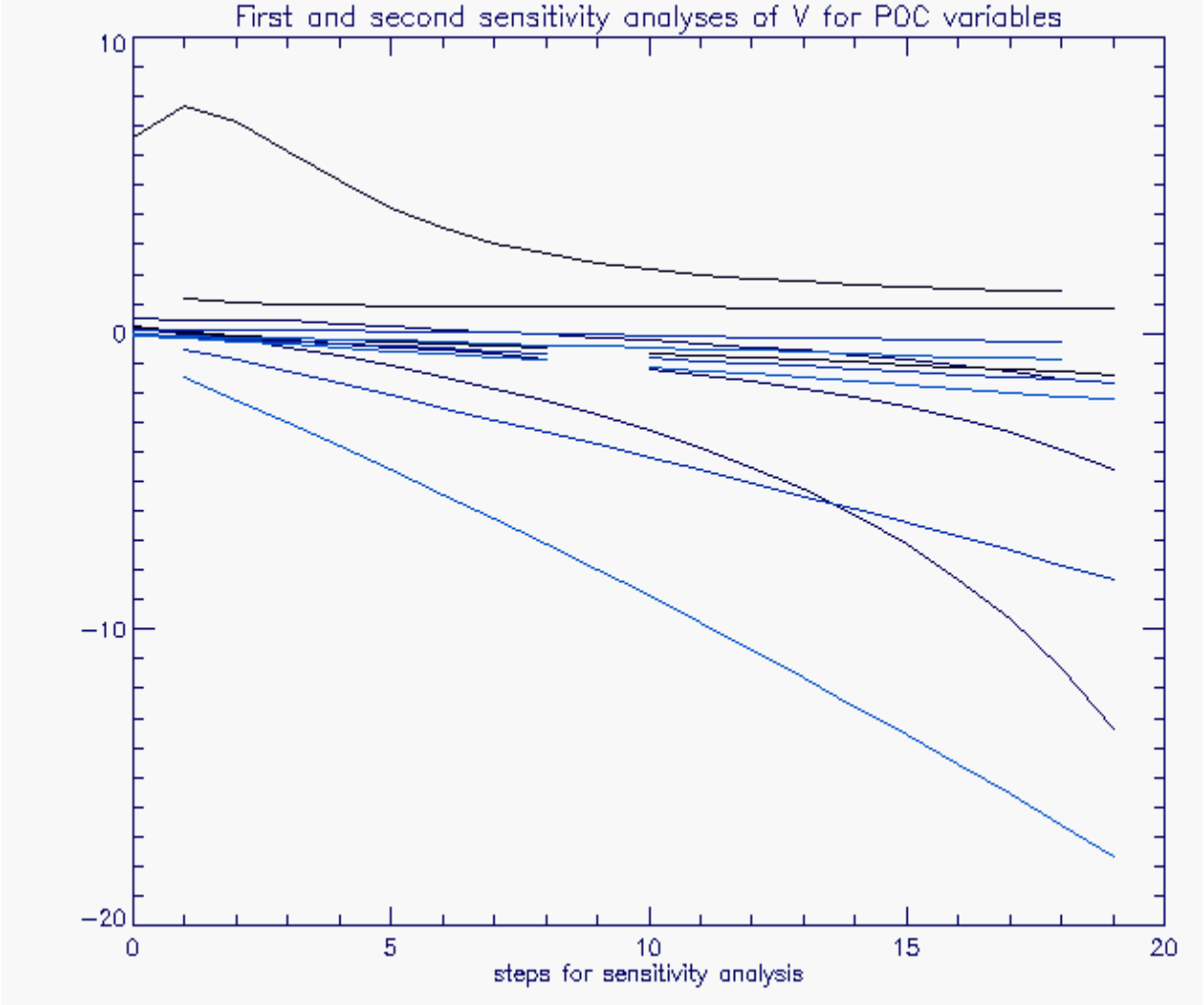

Figure 17: Plot of sensitivities for POC variables on sinking velocity. The same colour scale is applied as in fig.16.

Maximal sensitivities are obtained for the pycnocline and bottom boxes, so the deepest compartments of the model whereas the mixed box always shows smaller sensitivity. The biggest correlation values are calculated for the minimum initial value of V in the sensitivity analysis, with values up to -20,0, indicating a high and almost linear correlation of V and POC variable. On another hand, the other sensitivity values indicate a strong but lower sensitivity of this parameter with POC, for maximal and optimal initial value. No specific trend appears in the second analysis.

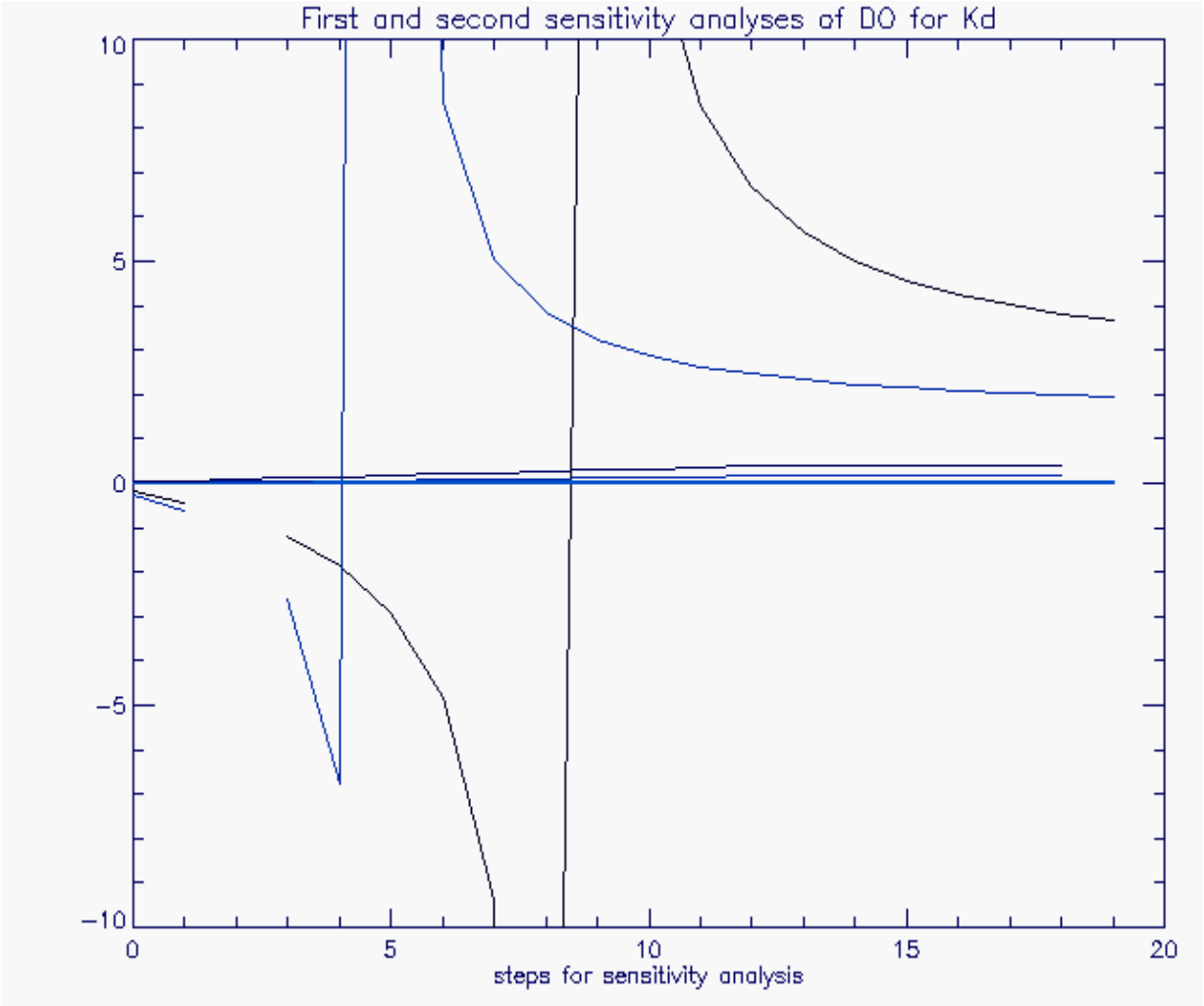

Figure 18: Sensitivity plots of oxidation rate with the different compartments of DO. The same colour scale is applied as in fig.16.

Almost all S_{DO} sensitivities show a low sensitivity of DO to Kd whatever the layer it should be, the biggest values are detected within pycno and bottom layers, for the maximum initial value. The local maxima for the other layers are not visible due to the low sensitivity and scale of DO variables to Kd. The second analysis shows some discrepancies especially in the local maximum and minimum (fig.19).

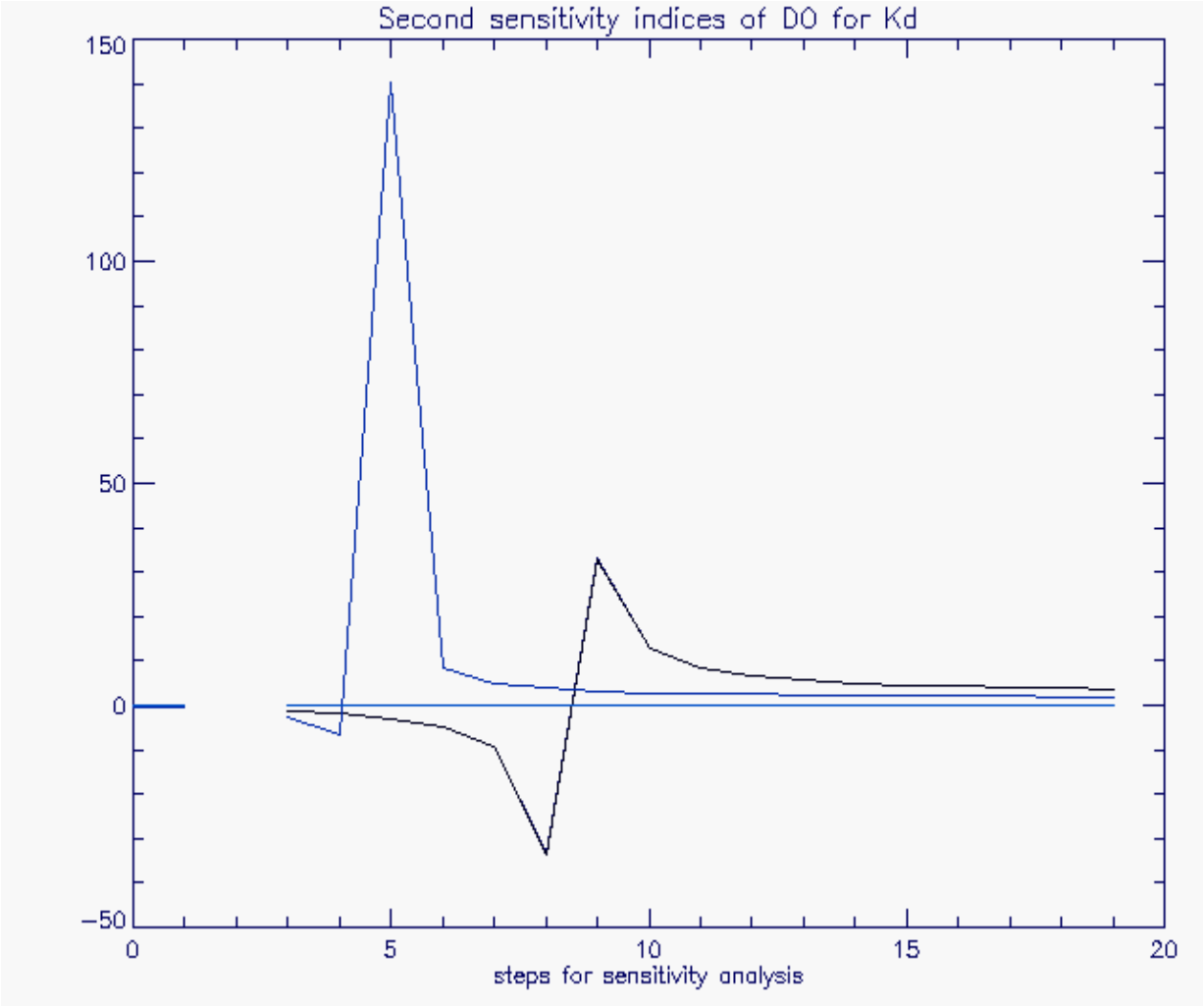

Figure 19: Sensitivity plots of second sensitivity analysis for oxidation rate with the different compartments of DO. The same colour scale is applied as in fig.16.

Values of maximum are higher than in the first analysis between -10.0 and +140.0 for the pycnocline layer and then -30.0/+30.0 for the bottom and sediment layers.

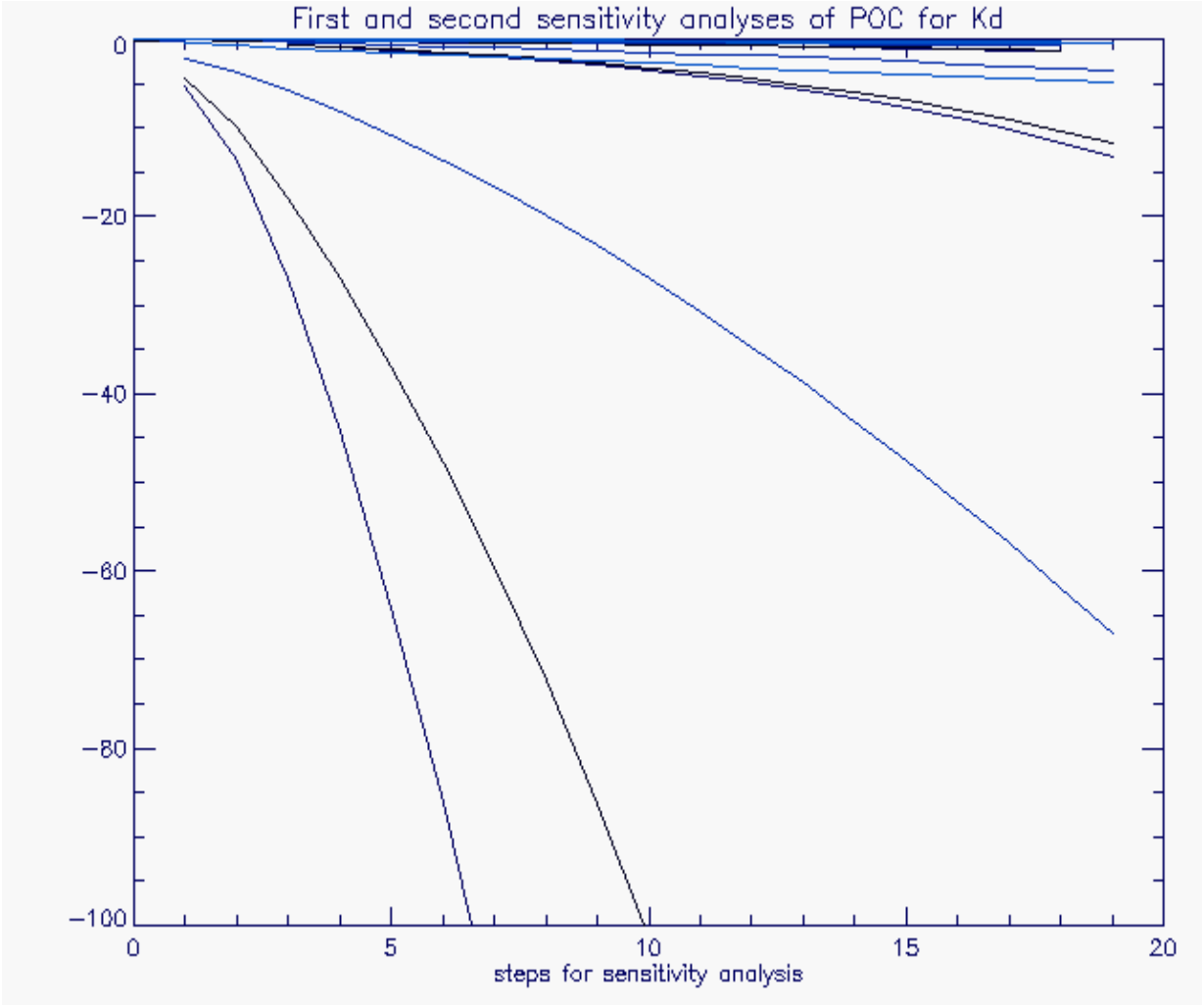

Figure 20: Sensitivity plots of oxidation rate with the different compartments of POC. The same colour scale is applied as in fig.16.

All S_{POC} sensitivities show a strong correlation between POC and Kd whatever the layer or compartment it should be. The sensitivities increased from the surface to the sediment layers, with biggest values detected for BL and SL. The maximum is reached with values up to -600.0 for the sensitivity analysis, performed on the minimum initial value, indicating a logarithmic correlation between oxidation rate and concentrations of carbon in the benthic layers. No specific tendency is coming out from the second analysis.

The major parameters or control variables for this global sensitivity analysis are correlated with the water variables and moreover with POC and to a less extent with DO. Generally the more correlated or influent parameters are oxidation rate and sinking velocity: Kd and V, with the strongest sensitivity values, whatever the optimal values tested.

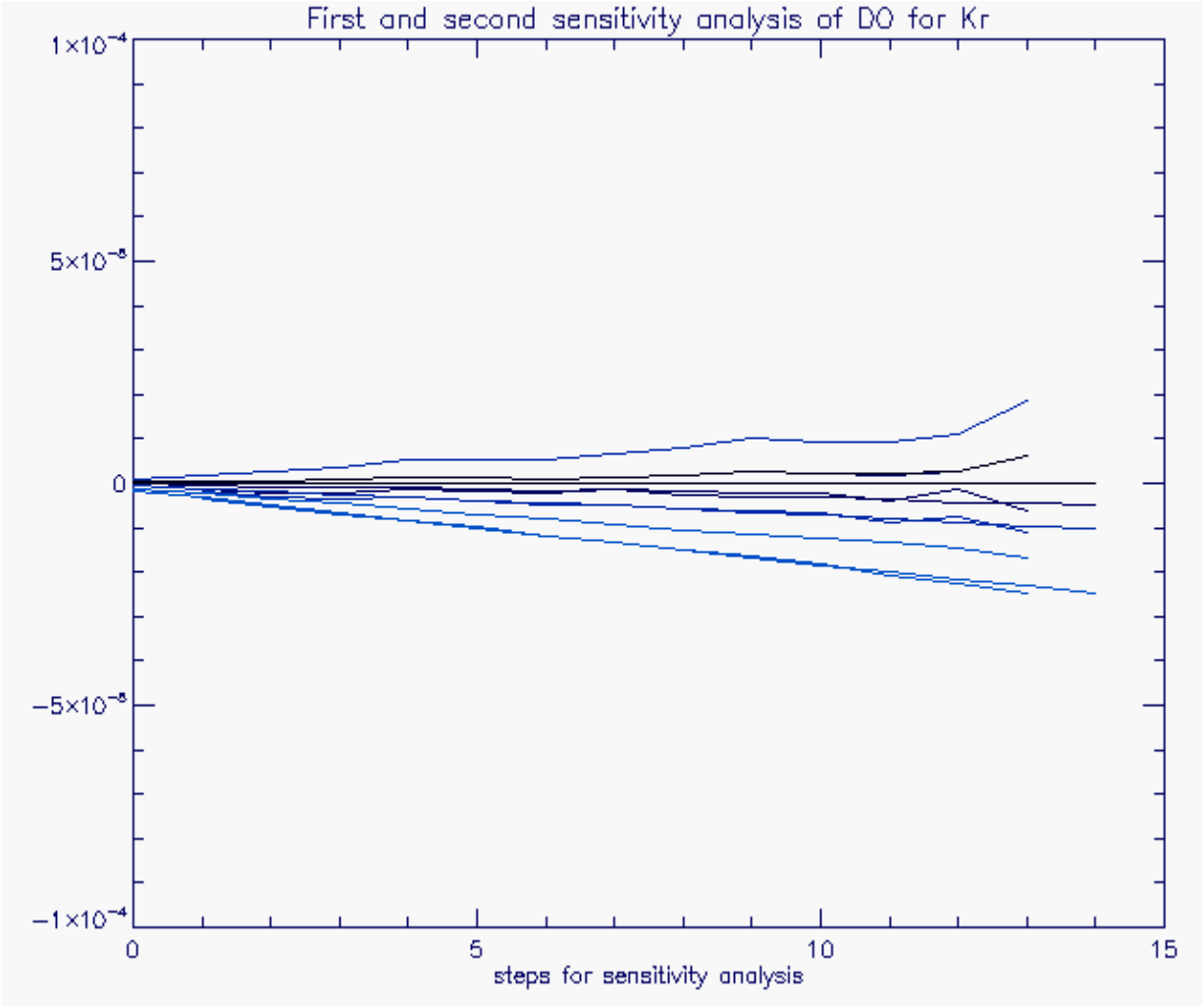

Figure 21: Sensitivity plots of Kr: respiration rate of primary producers and other organisms on oxygen product, for the different compartments of DO. Colour scale for S_{DO} plots is going from light blue for ML, to dark blue for PL and black for BL.

The highest values of sensitivity calculated were found in ML and PL, but they are very small, close to the lower sensitivity analysis. Whatever is the type of initial values in the sensitivity analysis, there is a weak correlation between these parameters and DO variables.

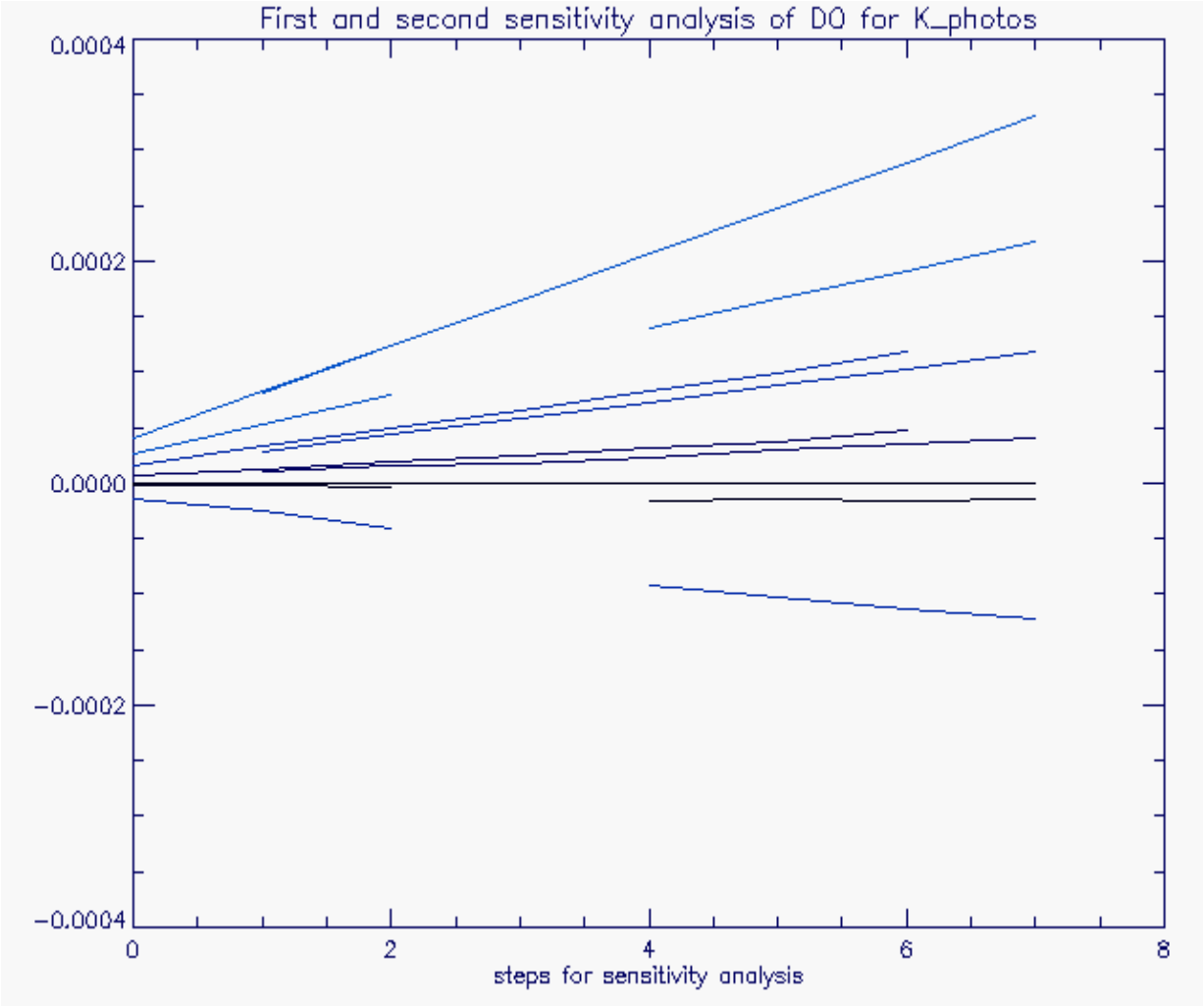

Figure 22: Sensitivity plots of Kphotos: photosynthetic conversion rate of primary producers for the different compartments of DO.

Kphotos shows a higher sensitivity compared to Kr with DO, even if weak compared to Kd and V. The higher values are found for the mixed and pycno layers.

Kr and Kphotos are inversely correlated, and only with oxygen variables, where the sensitivity values are weak, whereas no correlation is found for POC variables. Their sensitivities are low even for the upper range boundary, in the different sensitivity analysis performed for DO or POC (fig. 21-22). Hence, these parameters can be neglected in the evolution or stability of the biogeochemical model.

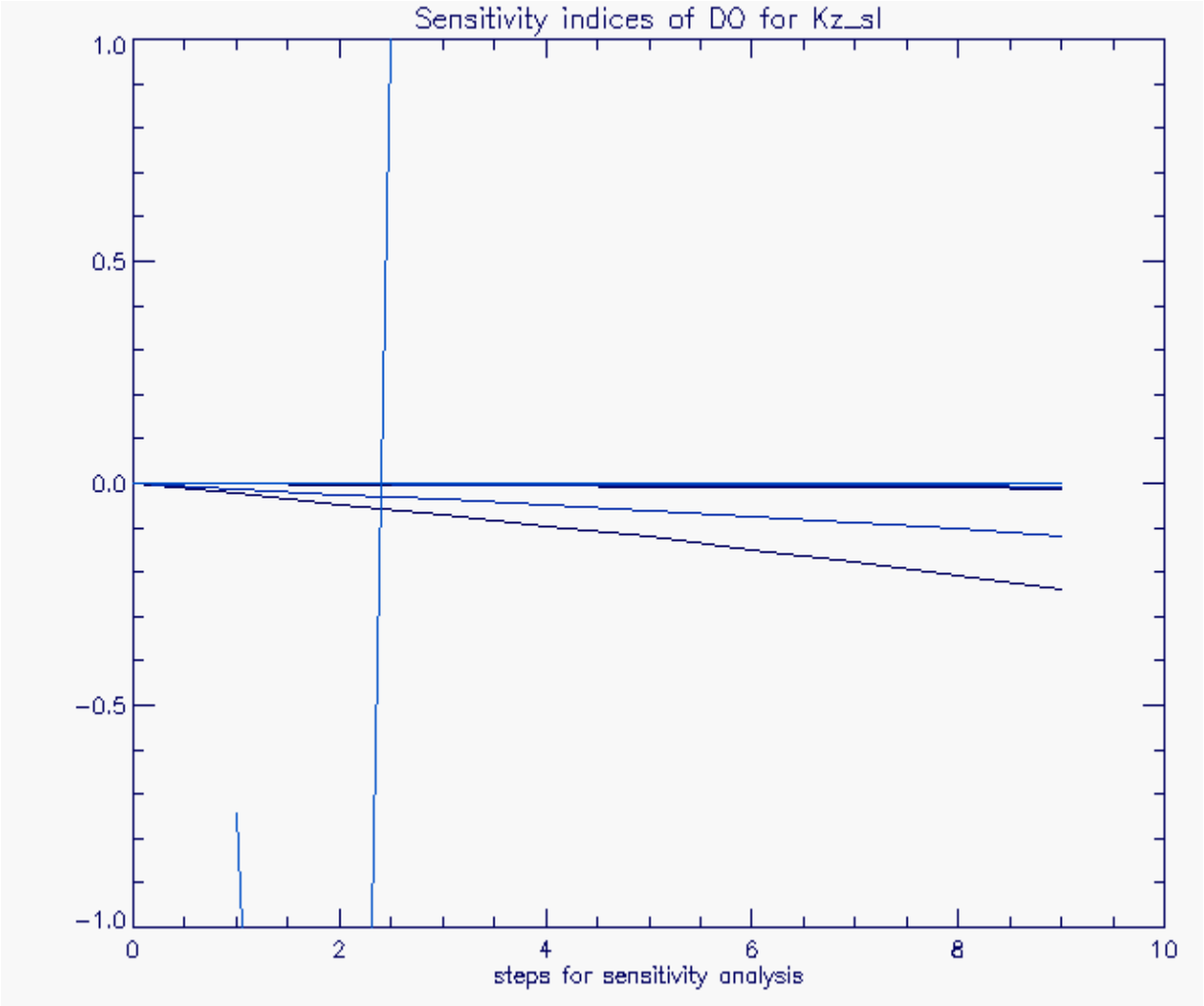

Figure 23: Plots of sensitivity index of DO variables, on Kz_sl: sediment-water diffusivity. The same colour scale as in fig.16 is applied.

The sensitivities increased from the surface to the bottom layers, with biggest values detected for BL. The maximum for the sensitivity analysis, performed on the maximal initial value, is obtained for S_{DO} in the benthic layer, indicating a higher sensitivity of Kz_sl. This sensitivity is rising in the second analysis with local maximum up to +6.0, but for pycno and bottom layers (cf. fig.24).

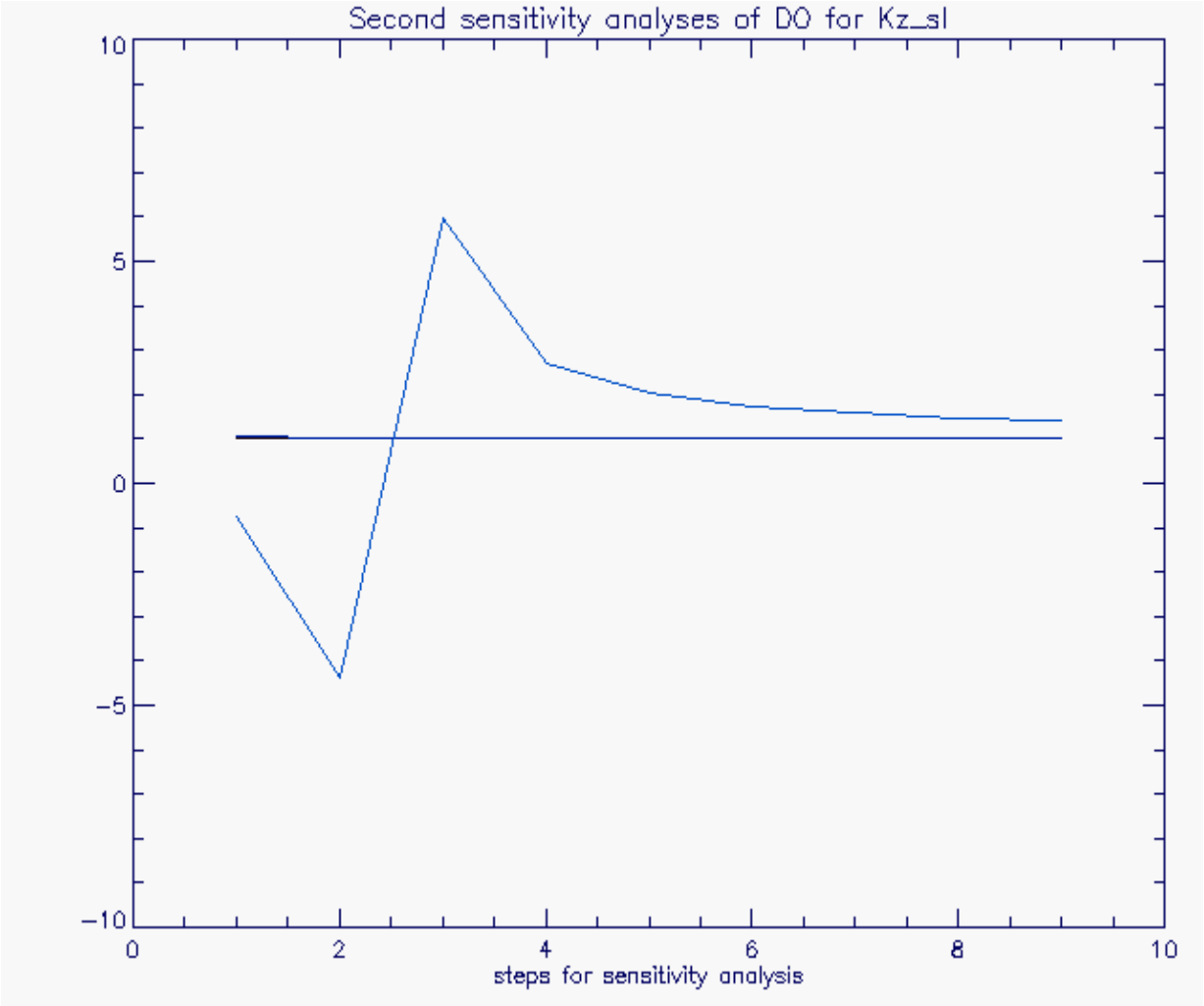

Figure 24: Plots of the second sensitivity analyses of DO variables, on Kz_sl. The same colour scale is applied as in fig.16.

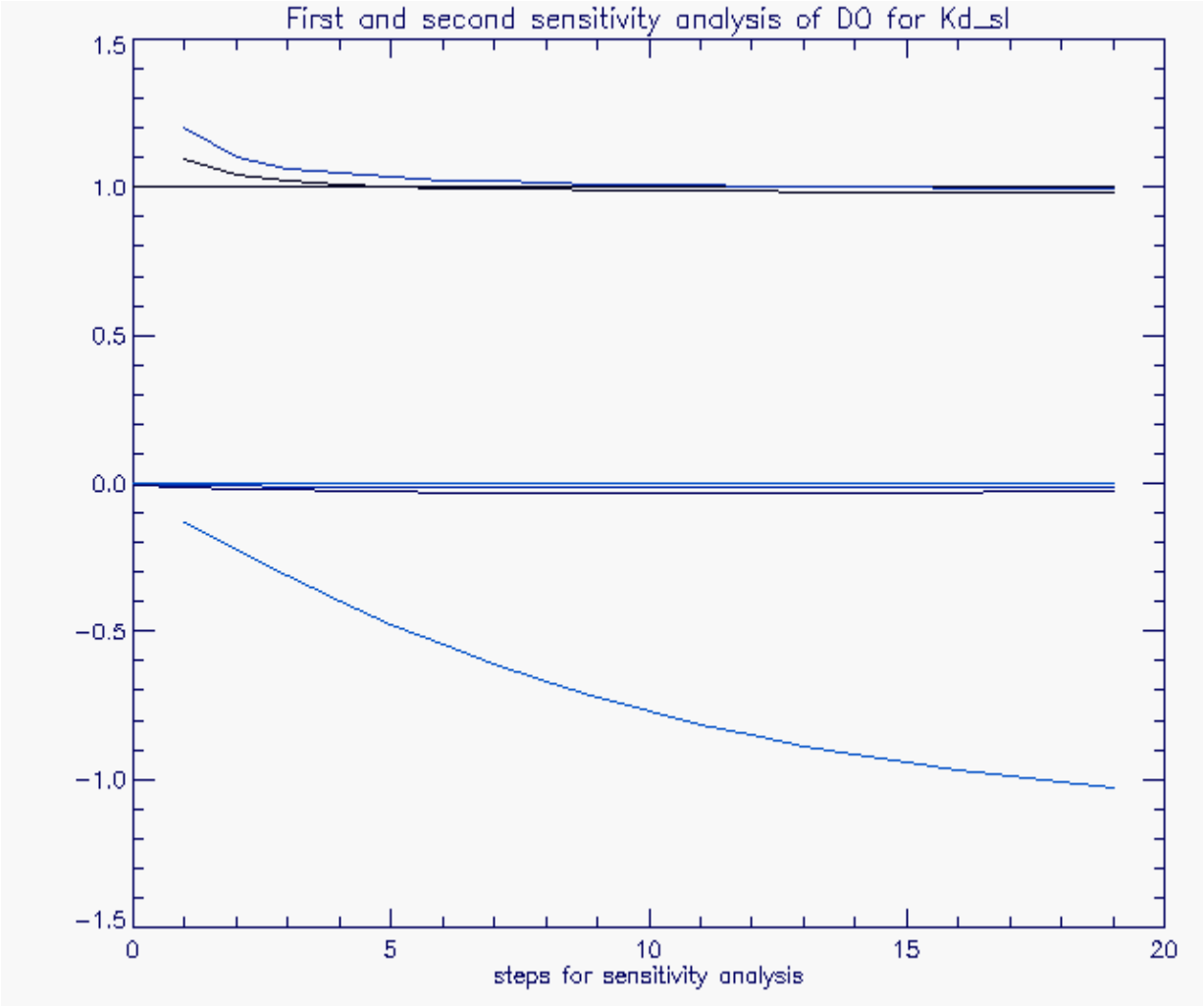

Figure 25: Plots of sensitivity index of DO variables, on Kd_sl: oxidation rate of carbon in sediment. The same colour scale as in fig.16 is applied.

For the sediment related parameters: Kz_sl, Kd_sl and POC_sl_t0, there is no effect on the POC variables except the sediment layer, in correlation with the sediment oxygen variable in the first sensitivity analysis (table 3, 4). Kz_sl, Kd_sl are correlated and evolved in parallel. Moreover, the sensitivities of these sediment-related parameters are low, and their correlation increase with the proximity or influence of the sediment layer. Therefore, the maximal sensitivity is found for the maximal value tested and the upper range boundary for pl DO and bl DO (fig.23-25). For the second analysis with unconstrained DO in sediment and bottom layers and a bigger zeta, Kz_sl and even Kd_sl constitute important parameters for the different DO variables with sensitivities close to those of Kd and V. This second analysis counterbalances the first one, and confirms the importance of Kz_sl and Kd_sl not only for sediment and bottom layer but for all DO variables. POC_sl_t0 displays always a low sensitivity or no effect on DO variable and sl POC. This parameter, as zeta, is independent of the other parameters or not visualized by sensitivity analysis. As zeta it only influences DO sl and DO bl, and their dynamic leading more or less rapidly to anoxia and hypoxia, when their optimal values are fixed.

V- CONCLUSIONS AND FURTHER WORK

5.1. FIRST CONCLUSIONS

The global sensitivity analysis highlighted the robustness of the model parameters, even when local maxima were detected as for Kd, V and Kz_sl (Friedrichs, 2001), the more influenced parameters of the sensitivity analysis on the state variables. Therefore, oxidation rate in water and sinking velocity are considered as the leading control variables (Garcia-Gorriz *et al.,* 2003) of the model, after the physical forcing functions. Considering the sediment compartment, we use the sediment-water diffusion rate as the third control variable, in our model, for the further steps of the model evaluation, especially due to its structure of sediment/pelagic coupled model.

For the physical variables or forcing functions, as primary production, some comparisons were performed between field and model data. Furthermore, we used this approach as we plan to apply this algorithm and usage of satellite data as a compulsory input for the biogeochemical application and development. This work would be further explained when fully validated for this area, on a latter stage. For salinity and temperature, the calibration or inter-comparisons between simulated and observed values, indicated for the first station of calibration a good correlation for temperature and seasonal cycle as dynamics. This work is a main part of calibration and validation stage and will be part of the next report (part B).

As a first conclusion on these physical forcing functions, we can state that the main error is coming from the time-lag between *in situ* and modelled results and an overestimation of bottom temperature and salinity in model compared to field measurements. As the hydrodynamic grid and dimension model are different from in situ stations sampling, we will use these modelled data as inputs for our 1D biogeochemical model, until its coupling with 3D hydrodynamic model. This source of errors can be considered as minor and included in the model uncertainty.

Actually, the main advantage of this model is its simplicity, as a 1D model it can be coupled with different types of hydrodynamic model, whatever the area of application; but the vertical dimension does not consider the advection or only indirectly through the temperature, salinity, primary production and diffusivity variations; which constitutes its main drawback. On the other hand, the biogeochemical model remains simple and easy to apply, as it is considering the carbon and oxygen in water and sediment and using model outputs and remote sensing data, at the European seas levels.

5.2 CALIBRATION

For these stations, the corresponding hydrodynamic and PP data are extracted and used for the running of the model.

For calibration, we firstly compare the weekly/monthly means, variance distribution and linear correlation coefficient of field/remote sensing data of PP for the first station chosen: Belt Sea.

Then comparisons of in situ/model temperature and salinity distributions and further correlation coefficient calculations are processed for the averaged boxes mixed, pycno and bottom layers, and corresponding pairs of data or sampling date.

Finally the calibration operation is performed following the formula of Jorgensen (1992) or Friedrichs (2001), on DO mixed layers, pycno layers and bottom layers, for daily averages but only for the matching days between observed and simulated values.
The cost-function is calculated using the following formula:

$$Y = \left[\frac{\Sigma \left(\frac{X_C - X_M}{X_{M,A}} \right)^2}{N} \right]^{1/2}$$

For Y the cost function of DO_{ML}, DO_{PL} and DO_{BL} on the one year run
X_C = the state variable computed value for the time t or daily mean,
X_M = the corresponding measured value for the time t or daily mean
$X_{M,A}$ = the average measured value corresponding to the annual mean
And N = number of measured-computed value pairs on the one year run

These differences are calculated and summed for the all run length and the different states variables in 1998. An optimization procedure is performed following each Y calculation, changing one parameter value and running the model, comparing for each run the Y calculated with the others. This optimization or minimization procedure is done until the cost-function reach a global minimum for the final model simulation results. This cost-function is calculated for each state variable and the optimization procedure is applied while varying the more sensitive and leading parameter model values, revealed by the sensitivity analysis (Jorgensen, 1992).

5.3 VALIDATION

For validation of the model, the same procedure as for calibration is performed but for in situ/simulation data and state variables of 2002, and the 8 stations.

Following, the comparisons of in situ/model data and cost-function, minimization calculation, a final regression analysis of the model results should be done, using the correlation coefficient with linear regression, and t-test to assess and finalize this validation.
In addition the calculation of residual error on the state variables allows a general estimation of the model fitting or accuracy (Jorgensen & Bendoricchio, 2002).

$$RE = \frac{\sum |obsvalues - simvalues|}{\sum |obsvalues|}$$

Obsvalues= for each or all DO variables, field measurements
Simvalues= for all or each DO variables, model results values, corresponding to the sampling dates of observed values
This operation is complementary of the regression and statistical analysis.

The next steps for the model validation so calibration and validation will be performed together with its further assessment in the Baltic, North and Adriatic Seas in parallel with further improvements or complexity increasing of its parameters and processes quantified.

AKNOWLEDGEMENTS

This work was performed under the ECOMAR institutional project of the JRC Framework Programme 6.
We wish to thank for their help and advices in the first stages of this work J. Cartensen[1], for his deep knowledge and experience of the Baltic Sea, E. Garcia-Gorriz[1] and Peter Bell[2] for their advices and help about modelling and model testing and F. Melin[1] & N. Hoepffner for providing the Sea-WiFS chlorophyll-a data processed and advices about the primary production algorithm and biogeochemical modelling.
The NERI and ICES provide us with the datasets used for calibration and comparison of simulated and in situ data.

[1] European Commission- Joint Research Centre, Institute for Environment and Sustainability
Inland & Marine Waters Unit, TP 272, I-21021 ISPRA (VA) – Italy

[2] C/-Georg Umgiesser, Oceanography, ISMAR-CNR, 1364 S. Polo, 30125 Venezia- Italy

REFERENCES

Arhonditsis G., Eleftheriadou M., Karydis M. & Tsirtsis G. Eutrophication risk assessment in coastal embayments using simple statistical models. 2003. Mar. Poll. Bull. 46, 1174-1178.

Baltic Sea Environment proceedings N 90. Thematic report. The 2002 oxygen depletion event in the Kattegat, Belt Sea and Western Baltic. 2003. Helsinki Commission Baltic Marine Enviroment Protection Commission.64 p.

Behrenfeld M.J. & Falkowski P.G. Photosynthetic rates derived from satellite-based chlorophyll concentration.1997. Limnol.Oceanogr.42(1),1-20.

Borsuk M.E., Stow C.A. & Reckhow K.H. A Bayesian network of eutrophication models for synthesis, prediction and uncertainty analysis. 2004. Ecol. Model. 173, 219-239.

Borsuk M.E., Stow C.A., Luettich R.A., Paerl H.W.& Pinckney J.L. Modelling oxygen dynamics in an intermittently stratified estuary: estimation of process rates using field data. 2001. Est, Coast. Shelf Sci. 52, 33-49.

Borsuk M.E., Higdon D., Stow C.A. & Reckhow K.H. A Bayesian hierarchical model to predict benthic oxygen demand from organic matter loading in estuaries and coastal zones. 2001. Ecol. Model. 143, 165-181.

Borum J. Shallow waters and land/sea boundaries. In Eutrophication in coastal marine ecosystems. 179-203. Jorgensen B.J. Richardson K. [Eds]. Coastal and estuarine studies. American Geophysical Union.

Bouman H.A., Platt T., Kraay G.W., Sathyendranath S. & Irwin B.D. Bio-optical properties of the subtropical North Atlantic.I. Vertical variability. 2000 a. Mar. Ecol. Prog. Ser. 200, 3-18.

Bouman H.A., Platt T., Sathyendranath S., Irwin B.D., Wernand M.R. & Kraay G.W. Bio-optical properties of the subtropical North Atlantic.II.Relevance to models of primary production. 2000 b. Mar. Ecol. Prog. Ser. 200, 19-34.

Burchard H., Bolding K. 2002. EUR 20253 EN. GETM A general estuarine Transport Model. Scientific Documentation. EC-JRC 157p.

Carlsson L., Persson J. & Hakanson L. A management model to predict seasonal variability in oxygen concentration and oxygen consumption in thermally stratified coastal waters. 1999. Ecol. Model. 119, 117-134.

Carstensen J., Conley D.J. & Muller-Karulis B. Spatial and temporal resolution of carbon ffluxes in a shallow coastal ecosystem, the Kattegat. 2003. MEPS, 252, 35-53.

Cloern, J.E., C. Grenz, and L. Vidergar-Lucas. 1995. An empirical model of the phytoplankton chlorophyll:carbon ratio – the conversion factor between productivity and growth rate. Limnol. Oceanogr. 40: 1313-1321.

Cloern J.E. 2001. Review. Our evolving conceptual model of the coastal eutrophication problem. Mar. Ecol. Prog. Ser. 210, 223-253.

Conley, D.J., Markager J., Andersen J., Ellerman T. & Svendsen L.M. 2002. Coastal eutrophication and the Danish National Aquatic Monitoring and Assessment Program. Estuaries 25, 706-719.

Cugier P. Modelisation du devenir a moyen terme dans l'eau et le sediment des elements majeurs (N, P, Si) rejetés par la Seine en Baie de Seine. 1999. Doctorat de L'université de Caen.270p.

Dadou I., Evans G. & Garcon V. Using JGOFS in situ and ocean color data to compare biogeochemicals models and estimate theirs parameters in the subtropical North Atlantic Ocean. J. Mar. Res., 65: 565-594. 2004.

Denman K.L. Modelling planktonic ecosystems: parameterizing complexity. 2003. Prog. Oceanogr. 57, 429-452.

Diaz R.J. J. Overview of hypoxia around the world. 2001. Environ. Qual. vol 30, 275-280.

Diaz R.J. & Rosenberg R. Overview of anthropogenically-induced hypoxic effects on marine benthic fauna. 129-146. In Coastal hypoxia: Consequences for living resources and ecosystems. Coastal and Estuarine Studies, 58. Rabalais Nancy N. and R. Eugene Turner [EDS.] American Geophysical Union, Washington D.C. 2001.

Djavidnia S., Druon J-N., Schrimpf W., Stips A., Peneva E., Dobricic S., Vogt P. Oxygen Depletion Risk Indices- OXYRISK & PSA V 2.0: New developments, structure and software content. 58p. EUR 21509 EN. 2005.

Dowell M. D., Campbell J.W., Moore T. S. Homogeneous biogeochemical provinces in a dynamic heterogeneous ocean. 2005. *In preparation*.

Druon J-N., Le Fèvre J. Sensitivity of a pleagic ecosystem model to variations of process parameters within a realistic range. J. Mar. Sys. 1999.

Druon J-N., Schrimpf W., Dobricic S. & Stips A. The physical environment as a key factor in assessing the eutrophication status and vulnerability of shallow seas: PSA & EUTRISK (V1.0). 2002. Report for European Commission, JRC EUR 20419 EN, Project COAST. 40p.

Druon J-N., Schrimpf W., Dobricic S. & Stips A. Comparative assessment of large-scale marine eutrophication: North Sea and Adriatic Sea as case studies. 2004. Mar. Ecol. Prog. Ser. Vol 272, 1-23.

Eppley R.W. 1972. Temperature and phytoplankton growth in the sea. Fishery Bulletin, 70, 1063-1085.

Feuerpfeil P., Rieling T., Estrum-Youseff R., Dehmlow J., Papenfuss T., Schoor A., Schiewer U. & Schubert H. Carbon budget and pelagic community compositions at two coastal areas that differ in their degree of eutrophication in the Southern Baltci Sea. Est. Caost. Shelf Sci. 61, 89-100. 2004.

Friedrichs, A.M. A data assimilative marine ecosystem model of the central equatorial Pacific: Numerical twin experiments. J.Mar.Res. 59, 859_894. 2001.

Garcia-Gorriz, E., Hoepffner N., Ouberdous M. Assimilation of SeaWIFS data in a coupled physical-biological model of the Adriatic Sea. J.Mar.Sys. 40-41, 233-252. 2003.

Gustafsson B. Time-dependant modeling of the Baltic entrance area. 1. Quantification of circulation and residence ties in the Kattegat and the straits of the Baltic sill. 2000. Estuaries, 23, 231-252.

Hamersley M.R. & Howes B.L. Contribution of denitrification to nitrogen, carbon, and oxygen cycling in tidal creek sediments of a New England salt marsh. 2003. Mar. Ecol. Prog. Ser. Vol 262, 55-69.

Harrison W.G., Platt T. & Lewis M.R. The utility of light-saturation models for estimating marine primary productivity in the field: A comparison with conventional "simulated" in situ methods. 1985. Can. J. Fish. Aquat. Sci. 42, 864-872.

Jassby A.D., J.E.Cloern & B.E.Cole. Annual primary production: Patterns and mechanisms of change in a nutrient-rich tidal ecosystem. 2002. Limnol.Oceanogr.47(3), 698-712.

Jorgensen B.B. 1996. Material flux in the sediment. In Eutrophication in coastal marine ecosystems. 115-135. Jorgensen B.J. Richardson K. [Eds]. Coastal and estuarine studies. American Geophysical Union.

Jorgensen B.B. 1996. Case study - Aarhus Bay. In Eutrophication in coastal marine ecosystems. 137- 155. Jorgensen B.J. Richardson K. [Eds]. Coastal and estuarine studies. American Geophysical Union.

Jorgensen SE. 1992. Ecology & Environment. Integration of ecosystem theories: a pattern. Kluwer, Dordrecht, Netherlands. 450 p.

Jorgensen S.E., Bendoricchio G. 2002. Developments in environmental modeling 21. Fundamentals of ecological modeling (3rd edition). Elsevier, Oxford, UK. 530 p.

Justic D., Rabalais N.N. & Turner R.E. Modeling the impacts of decadal changes in riverine nutrient fluxes on coastal eutrophication near the Mississippi river delta. 2002. Ecol. Model. 152, 33-46.

Kabuta S.H. & Laane R.W.P.M. Ecological performance indicators in the North Sea: development and application. 2003. Ocean & Coastal Management. 46, 277-297.

Karydis M., Tsirtsis G. Ecological indices: a biometric approach for assessing eutrophication levels in the marine environment; Sci. Tot. Env. 186, 209-219. 1996.

Moll A. & Radach G. Review of three-dimensional ecological modeling related to the North-Sea shelf system. Part 1: models and their results. 2003. Prog Oceano. 57, 175-217.

Moncheva S., Gotsis-Skretas O., Pagou K. & Krastev A. 2001.Phytoplankton blooms in Black Sea and Mediterranean coastal ecoxyxtems subjected to anthropogenic eutrophication : similarities and differences. Est. Coast. Shelf Sc. 53, 281-295.

Moncheva S., Doncheva V., Shtereva G., Kamburska L., Malej A. & Gorinstein S. 2002.Application of eutrophication indices for assessment of the Bulgarian Black Sea coastal ecosystem ecological quality. Water Science and Technology. Vol 46, 19-28.

Neumann T. Towards a 3D-ecosystem model in the Baltic Sea. 2000. J. Mar. Sys. 25, 405-419.

Neumann T., Fennel W. & Kremp C. Experimental simulations with an ecosystem model of the Baltic Sea: a nutrient load reduction experiment. 2002. Global Biogeo. Cycles,16, 18p.

Nixon S. C. Coastal marine eutrophication: a definition, social causes, and future concerns. 1995. Ophelia, vol 41, 199-219.

Paerl H.W., Pinckney J.L., Fear J.M. & Peierls B.L. 1998. Ecosystem responses to internal and watershed organic matter loading: consequences for hypoxia in the eutrophying Neuse River Estuary, North Carolina, USA. Mar. Ecol. Prog. Ser. 166, 17-25.

Platt, T. and Sathyendranath, S. 1993. Estimators of primary production for interpretation of remotely sensed data on ocean color. *J. Geophys. Res.,* **98:** 14,561-14,576.

Rabalais N. N. and R. E. Turner. 2001. Hypoxia in the Northern Gulf of Mexico: description, causes and change. 1-36. In Coastal hypoxia: Consequences for living resources and ecosystems. Coastal and Estuarine Studies, 58. Rabalais Nancy N., and R. Eugene Turner [EDS.] American Geophysical Union, Washington D.C. vii+ 463p.

Rice J. Environmental health indicators. 2003. Ocean & Coastal Management. 46, 235-259.

Richardson K. & Jorgensen B.B. Eutrophication: definition, history and effects. 1996. In Eutrophication in coastal marine ecosystems. 1-20. Jorgensen B.J. Richardson K. [Eds]. Coastal and estuarine studies. American Geophysical Union.

Richardson K. Carbon flow in the water column case study: the Southern Kattegat.1996. In Eutrophication in coastal marine ecosystems. 95-114. Jorgensen B.J. Richardson K. [Eds]. Coastal and estuarine studies. American Geophysical Union.
Riegman R. Nutrient-related selection mechanisms in marine phytoplankton communities and the impact of eutrophication on the planktonic food web. 1995. Wat. Sci. tech, vol 32, n 4, 63-75.

Soetaert K., Herman P.M.J., Middelburg J.J. 1996 a. Dynamic response of deep-sea sediments to seasonal variations : a model; Limnol. Oceanogr. 41(8), 1651-1668.

Soetaert K., Herman P.M.J., Middelburg J.J. 1996 b. A model of early diagenetic processes from the shelf to abyssal depths. Geoch. Cosmochim. Acta. 60(6), 1019-1040.

Soetaert K., Herman P.M.J., Middelburg J.J., Heip C. 1998. Assessing organic matter mineralization, degradability and mixing rate in an ocean margin sediment (Northeast Atlantic) by diagenetic modeling. J.Mar. Res. ,56, 519-534.

Soetaert K., Middelburg J.J., Herman P.M.J., Buis K. 2000. On the coupling of benthic and pelagic biogeochemical models. Earth-Sicence Rev. 51, 173-201.

Soetaert K., Herman P.M.J., Middelburg J.J., Heip C., Smith C.L., Tett P., Wild-Allen K. 2001. Numerical modelling of the shelf break ecosystem: reproducing benthic and pelagic measurements. Deep-Sea Res., 48, 3141-3177.

Stips A., Bolding K., Pohlmann T. & Burchard H. 2004. Simulating the temporal and spatial dynamics of the North Sea using the new model GETM (general estuarine transport model). Ocean Dynamics. 54, 266-284.

Tett P., Gilpin L., Svendsen H., Erlandsson C.P., Larsson U., Kratzer S., Fouilland E., Janzen C., Lee J-Y., Grenz C., Newton A., Ferreira J-G., Fernandes T. & Scory S. 2003. Eutrophication and some European waters restricted exchange. Cont. Shelf Res. 23, 1635-1671.

Turner R.E., Rabalais N.N., Swenson E.M., Kasprzak M. & Romaire T. 2005. Summer hypoxia in the Northern Gulf of Mexico an its prediction from 1978 to 1995. Mar. Env. Res. 59, 65-77.

UNESCO. Tenth report on oceanographic tables ans standards. UNESCO Technical Papers in Marine Research. UNESCO, Paris. 1981.

Vichi M., Oddo P., Zavaterelli M., Coluccelli A., Coppini G., Celio M., Fonda Umnai S. & Pinardi N. 2003. Calibration and validation of a one-dimensional complex marine biogeochemical flux model in different areas of the northern Adriatic shelf. Annales Geophysicae 413-436.

Vidal M., Duarte C. M. & Sanchez C. Coastal eutrophication research in Europe: progress and imbalances. 1999. Mar. Poll. Bull., vol 38, n 10, 851-854.

Vollenweider R. A. Coastal marine eutrophication: principles and control. 1992. 1-21.Marine Costal Eutrophication, The response of Marine Transitional Systems to human impact: problems and perspectives for restoration. Vollenweider R.A., Marchetti, R., Viviani R. [Eds]. Elsevier, Amsterdam, reprinted from Sc.Tot. Env., supplement 1992.

Vollenweider R., Giovanardi F., Montanari G. & Rinaldi A. 1998. Characterization of the trophic conditions of marine coastal waters with special reference to the North West Adriatic Sea, proposal for a trophic scale, turbidity and generalized water quality index., Environmetrics, vol 9, pp 329-357.

Weiss R.F. The solubility of nitrogen, oxygen, and argon on water and sea-water. 1970. Deep-Sea Res., 17, 721-735.

Wool T.A., Ambrose R.B., Martin J.L., Comer E.A. WASP version 6. User's manual. EPA website. 2002-2003. chap 3-4, 7-9.

Zaldivar J.M., Cattaneo E., Plus M., Murray C.N., Giordani G. & Viaroli P. 2003.Long-term simulation of main biogeochemical events in a coastal lagoon: Sacca di Goro (Northern Adriatic Coast, Italy). Cont. Shelf Res. 23, 1847-1875.